

**Pharmacological manipulation of the glutamate transporter
system in health and disease**

by © Crystal M. Wilkie

A Thesis submitted to the School of Graduate Studies in partial fulfilment of the requirements for the degree of **Master of Science in Medicine (Neuroscience)**.

Division of BioMedical Sciences/Faculty of Medicine

Memorial University of Newfoundland

October 2019

St. John's Newfoundland and Labrador

Abstract

Glutamate transporter-1 (GLT-1) is the main glutamate transporter in the brain. Dysfunctional GLT-1 has been suggested to cause glutamate uptake impairments in Huntington disease (HD). It is thought that simply increasing GLT-1 expression can increase glutamate uptake in the brain. However, the functional effect of increasing GLT-1 expression in HD or the healthy brain has not been studied. We increased GLT-1 expression using two compounds, ceftriaxone and LDN/OSU-0212320 (LDN), and used the iGluSnFR technique to visualize glutamate dynamics in real-time. We found an impairment in glutamate uptake in the HD hippocampus in mice that was surprisingly not alleviated by ceftriaxone treatment. Furthermore, we found that increasing GLT-1 expression through ceftriaxone or LDN treatment in the healthy brain had no effect on glutamate uptake. These results suggest that increasing glutamate uptake is much more complex than just increasing GLT-1 expression.

ACKNOWLEDGMENTS

First and foremost, I would like to thank my supervisor Dr. Matthew Parsons for his never-ending support and guidance. He took a chance on me as a graduate student when no one else would even speak to me; for that I am ever grateful.

I would like to thank our research assistant, Firoozeh Nafar, for her positivity, support, and her help in teaching me how to perform western blots.

I also have the utmost appreciation for my lab mates. Thank you for performing dissections for me when I was hesitant about sacrificing mice and for making the lab fun every single day.

Finally, I would like to thank the other graduate students for their guidance and help with imposter syndrome, as well as my family for always providing me with love and support.

Chapter 1 Table of Contents

Chapter 1 Introduction	1
1.1 An Introduction to Glutamate Neurotransmission	1
1.1.1 Glutamate transporters	5
1.1.2 GLT-1 and Glutamate Clearance	8
1.2 Methods to research glutamate dynamics	10
1.2.1 Microdialysis.....	10
1.2.2 Synaptically-Activated Transporter Currents	10
1.2.3 Biochemical Uptake Assay	11
1.2.4 Fluorescent Biosensor of Glutamate	11
1.3 An Introduction to Huntington Disease	12
1.3.1 Symptoms and Treatment	13
1.3.2 Mouse models of HD	14
1.3.3 Glutamate uptake and GLT-1 in HD	17
1.3.4 Long-Term Potentiation (LTP) and HD.....	20
1.4 Pharmacological ways to increase GLT-1 expression	22
1.5 Aims and Hypothesis	23
Chapter 2: Materials and Methods	24
2.1 Animals and Drugs.....	24

2.2	Stereotaxic Surgery	25
2.3	Slice Preparation	26
2.4	Imaging and image analysis	27
2.5	Electrophysiology for experiment 1 (HFS LTP).....	28
2.6	Western Blots	29
2.7	Statistics	30
Chapter 3 Results		31
3.1	Experiment 1: Treating an animal model of HD with ceftriaxone.....	31
3.1.1	Characterization of extracellular glutamate dynamics in the hippocampus during HFS	31
3.1.2	Characterization of glutamate dynamics in the hippocampus during TBS..	35
3.1.3	GLT-1 expression in hippocampal tissue from WT and Q175FDN mice ...	38
3.1.4	HFS LTP experiments.....	41
3.2	Experiment 2: Pharmacologically increasing GLT-1 expression in the healthy brain.....	41
3.2.1	Glutamate Clearance in the Cortex after GLT-1 Upregulation.....	42
3.2.2	Glutamate Clearance in the Hippocampus after GLT-1 Upregulation	49
3.2.3	Glutamate Clearance in the Striatum after GLT-1 Upregulation.....	55
Chapter 4 Discussion		61

4.1	Using ceftriaxone to treat the Q175FDN mouse model of HD.....	61
4.1.1	Glutamate Dynamics in the Hippocampus during HFS and TBS stimulation.....	61
4.1.2	Ceftriaxone does not Alleviate LTP Impairments in HD and Impairs LTP in WT Mice.....	63
4.1.3	Ceftriaxone did not increase GLT-1 expression in aged animals	64
4.2	Pharmacologically increasing GLT-1 expression in the brain	65
4.2.1	Ceftriaxone Treatment to Increase GLT-1 Expression.....	66
4.2.2	LDN Treatment to Increase GLT-1 Expression.....	69
4.3	Conclusion.....	70
	REFERENCES	71
	APPENDIX.....	94

List of Tables

Table 1.1 Summary of HD mouse models.....	18
---	----

List of Figures

Figure 1.1 Schematic of a Tripartite Synapse.....	2
Figure 1.2 Glutamate Clearance Impairments can Cause a Spillover Effect.....	6
Figure 3.1 Characterization of glutamate dynamics in the hippocampus during HFS	33
Figure 3.2 Characterization of glutamate dynamics in the hippocampus during TBS	36
Figure 3.3 GLT-1 expression.....	39
Figure 3.4 Characterization of glutamate dynamics in the cortex after ceftriaxone treatment.	44
Figure 3.5 Characterization of glutamate dynamics in the cortex after LDN treatment.....	47
Figure 3.6 Characterization of glutamate dynamics in the hippocampus after ceftriaxone treatment.	50
Figure 3.7 Characterization of glutamate dynamics in the hippocampus after LDN treatment.	53
Figure 3.8 Characterization of glutamate dynamics in the striatum after ceftriaxone treatment	56
Figure 3.9 Characterization of glutamate dynamics in the striatum after LDN treatment.	59

List of Abbreviations

°C: Degrees Celsius

%: Percent

μA: Microampere

μl: Microlitre

μM: Micromolar

3-NPA: 3-Nitropropionic acid

AD: Alzheimer disease

ACSF: Artificial cerebral spinal fluid

ALS: Amyotrophic lateral sclerosis

AMPA: α -amino-3-hydroxy-5-methyl-4-isoxazolepropionic acid

AMPA: α -amino-3-hydroxy-5-methyl-4-isoxazolepropionic acid receptor

APS: Ammonium persulfate

BSA: Bovine serum albumin

BME: Beta- mercaptoethanol

Ca²⁺: Calcium

CAG: Cytosine-Adenine-Guanine

CaMKII: Calmodulin-dependent protein kinase II

Cef: Ceftriaxone

Cl⁻: Chlorine

CNS: Central nervous system

DMSO: Dimethylsulfoxide

DTBZ: Deutetrabenazine

EAAT1: Excitatory amino acid transporter 1

EAAT2: Excitatory amino acid transporter 2

EAAT3: Excitatory amino acid transporter 3

EAAT4: Excitatory amino acid transporter 4

EAAT5: Excitatory amino acid transporter 5

EPSCs: Excitatory postsynaptic currents

ERK: Extracellular-signal regulated kinase

ex-NMDARs: Extrasynaptic NMDARs

F/F: Fluorescence/ fluorescence

FDA: Food and Drug Administration

fEPSP: field excitatory post-synaptic potential

GABA: Gamma-aminobutyric acid

GFAP: Glial fibrillary acidic protein

GFP: Green fluorescent protein

GLAST: Glutamate aspartate transporter

GLT-1: Glutamate transporter-1

H&E: Haematoxylin & Eosin

HD: Huntington disease

HET: Heterozygous

HFS: High frequency stimulation

HOM: Homozygous

HTT: Huntingtin gene

Htt: Huntingtin protein

Hz: Hertz

IB: Inclusion bodies

iGluSnFR: Intensity-based glutamate sensing fluorescent reporter

i.p.: Intraperitoneal

IOS: Intrinsic Optical Signal

IT15: Interesting transcript 15

K⁺: Potassium

Kt: Transport affinity

LED: Light-emitting diode

LTP: Long term potentiation

Mg²⁺: Magnesium

mGluR: Metabotropic glutamate receptor

mHtt: Mutant huntingtin

mM: Millimolar

mRNA: Messenger RNA

ms: Millisecond

Na⁺: Sodium

NF- κ B: Nuclear factor-kappaB

nM: Nanomolar

NMDA – *N*-methyl-*D*-aspartate

NMDAR: *N*-methyl-*D*-aspartate receptor

PKA: Protein kinase A

PKC: Protein kinase C

ROI: Region of interest

RM ANOVA: Repeated measure ANOVA

RT-PCR: Reverse transcription-polymerase chain reaction

s.c.: Subcutaneous

Sal: Saline

siRNA: Small interfering RNA

STC: Synaptically-activated transporter current

syn-NMDARs: Synaptic NMDARs

TBS: Theta burst stimulation

TBS-T: Tris-buffered saline-Tween20

TBZ: Tetrabenazine

VMAT: Vesicular monoamine transporters

WT: Wild-type

YAC: Yeast artificial chromosome

Yb-1: y-box-binding protein 1

CO-AUTHORSHIP STATEMENT

I, Crystal Wilkie, am first author of this manuscript. I performed all of the experiments except for the HFS LTP experiments which are shown in the Appendix (Figure A1).

These HFS-LTP data were completed by our honours student Cherry-Lynn Benson and were obtained from animals that I had treated with saline or ceftriaxone.

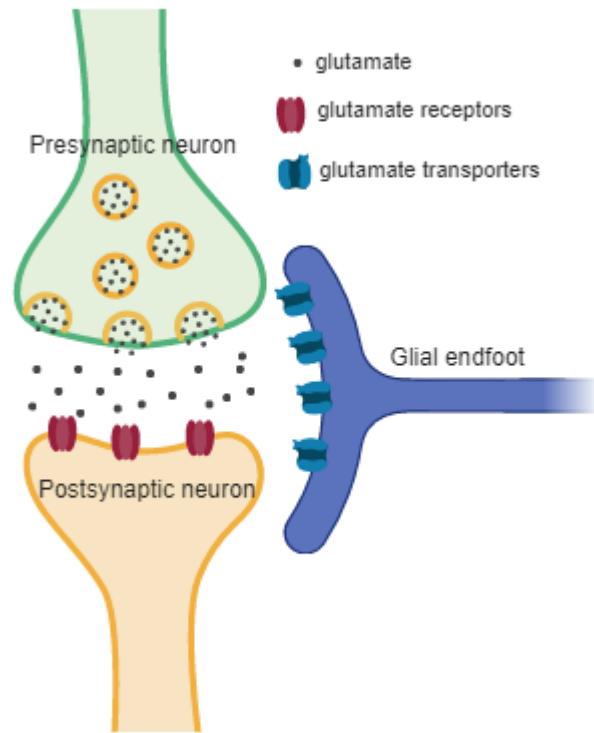
Chapter 1 Introduction

1.1 An Introduction to Glutamate Neurotransmission

Glutamate, an amino acid, is the brain's most abundant excitatory neurotransmitter. Glutamatergic synapses are typically tripartite synapses containing a presynaptic neuron, postsynaptic neuron, and a surrounding glial cell (Figure 1.1). During typical glutamate neurotransmission, synaptic vesicles containing glutamate fuse with the presynaptic membrane and glutamate is released into the extracellular space via exocytosis (Naito & Ueda, 1983; Cousin & Robinson, 1999). Once in the synaptic cleft, glutamate can bind to glutamate receptors which can be ionotropic or metabotropic and located on either the pre- and/or post-synaptic membranes (Reiner & Levitz, 2018). Ionotropic glutamate receptors include α -amino-3-hydroxyl-5-methyl-4-isoxazole-propionate (AMPA), kainate, and N-methyl-D-aspartate (NMDA) receptors. Metabotropic receptors are subdivided into three groups: group I (mGluR1, mGluR5) are mainly located postsynaptically and responsible for enhancing neuronal excitability; group II (mGluR2 and mGluR3) are located on presynaptic and postsynaptic membranes and are involved in inhibiting neurotransmitter release; and group III (mGluR4, mGluR6, mGluR7, and mGluR8) serve the same function as group II except they are predominately located on postsynaptic membranes in the cerebellum (Niswender & Conn, 2010).

AMPA receptors (AMPA receptors) are tetramers that consist of various combinations of four distinct subunits; GluA1-GluA4 (Song & Huganir, 2002). These receptors are typically permeable to Na^+ , K^+ , and can be permeable to Ca^{2+} ; however, Ca^{2+} ion influx is prevented by the presence of a GluA2 subunit (Man, 2011). AMPARs exhibit rapid

Figure 1.1 Schematic of a Tripartite Synapse. There are three main aspects to a tripartite synapse; a presynaptic neuron which releases glutamate, a postsynaptic neuron where the glutamate receptors are located, and a surrounding glial cell responsible for removing excess neurotransmitter. Image created using Biorender.



presence of a GluA2 subunit (Man, 2011). AMPARs also exhibit rapid activation and inactivation kinetics, with AMPAR-mediated excitatory postsynaptic currents (EPSCs) decaying within milliseconds (Colquhoun et al., 1992; Hestrin, 1992; Clements et al., 1998).

Compared to AMPARs, NMDARs have slow activation and inactivation kinetics, high permeability to Ca^{2+} , and a Mg^{2+} blockage at resting membrane potential (Dzubay & Jahr, 1996). To activate NMDARs three events must occur: glutamate binding, removal of Mg^{2+} blockade by postsynaptic depolarization, and binding of either glycine or D-serine which are co-agonists (Dore et al., 2017; Traynelis et al., 2010). Due to their slow inactivation kinetics and high affinity for glutamate (Traynelis et al., 2010), these receptors show a longer duration EPSC than AMPARs (Lester & Jahr, 1992).

Structurally, these receptors are heterotetramers that consist of two obligatory GluN1 subunits plus any combination of GluN2A-D and/or GluN3A-B subunits (Traynelis et al., 2010). NMDARs can be located synaptically (syn-NMDARs) as well as extrasynaptically (ex-NMDARs) on the postsynaptic neuron, and can also exist presynaptically (Hardingham & Bading, 2010; Banerjee et al., 2015).

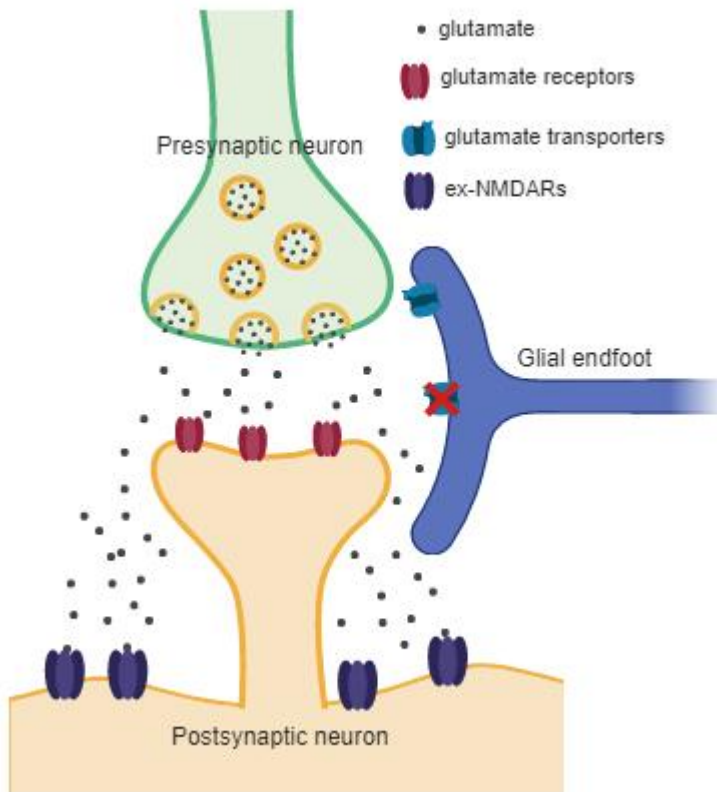
While glutamate is necessary for fast excitatory neurotransmission and for many forms of activity-dependent synaptic plasticity (Danbolt, 2001; Fonnum, 1984; Ottersen & Storm-Mathisen, 1984), glutamate can accumulate in the extracellular space to toxic levels if not properly regulated. An accumulation of glutamate leads to a spillover effect which can activate ex-NMDARs and is thought to cause synaptic plasticity impairments (Li et al., 2011) and cell death (Hardingham & Bading, 2010; Parsons and Raymond,

2014) as shown in Figure 1.2. Efficient transporter-mediated glutamate uptake is required to prevent this excitotoxicity (Danbolt, 2001; Parsons & Raymond, 2014).

1.1.1 Glutamate transporters

Glutamate transporters are sodium-dependent transporters that are located on both neurons and astrocytes (Rothstein et al., 1994; Danbolt, 2001). Currently, there are five known glutamate transporters. Glutamate transporter-1 (GLT-1, also known as excitatory amino acid transporter 2 or EAAT2) is the brain's most abundant transporter and is primarily located on astrocytes (Danbolt et al., 1992; Tanaka et al., 1997; Otis & Kavanaugh, 2000). It is expressed brain-wide with the highest concentrations observed in the hippocampus and neocortex (Danbolt et al., 1992; Levy et al., 1993). Another glutamate transporter, called glutamate aspartate transporter (GLAST; also known as excitatory amino acid transporter 1 or EAAT1), is also highly expressed on astrocytes throughout the brain with a higher concentration of transporter expression levels detected in the cerebellum (Rothstein et al., 1995; Schmitt et al., 1997; Berger & Hediger, 1998). Excitatory amino acid transporter 3 (EAAT3) is predominately expressed on neuronal membranes while excitatory amino acid transporter 4 (EAAT4) is found on neuronal membranes in the cerebellum (Rothstein et al. 1994; Shashidharan et al., 1997; Dehnes et al., 1998; Holmseth et al., 2012). Excitatory amino acid transporter 5 (EAAT5) has low expression levels in the brain and is predominately located on retinal photoreceptors and bipolar cells (Fairman et al., 1995). Despite the widespread presence of multiple glutamate transporters throughout much of the neuroaxis, GLT-1 is thought to be the most

Figure 1.2 Glutamate Clearance Impairments can Cause a Spillover Effect. If glutamate transporters, in particular GLT-1, are dysfunctional or downregulated then glutamate clearance is impaired. This causes an accumulation of glutamate in the extracellular space that spills over and activates ex-NMDARs. Image created using Biorender.



important transporter involved in glutamate clearance (Danbolt et al., 1992; Tanaka et al., 1997; Otis & Kavanaugh, 2000).

1.1.2 GLT-1 and Glutamate Clearance

GLT-1 co-transporters one molecule of glutamate, three molecules of Na^+ and one H^+ into the cell and counter-transporters one molecule of K^+ with each cycle (Wadiche et al., 1995; Danbolt 2001). GLT-1 is a homomer that is composed of three subunits in a bowl shape with the glutamate binding site located at the bottom of the bowl (Yernool et al., 2004; Tzingounis & Wadiche, 2007). When glutamate and the co-transported ions are not bound to the transporter, the glutamate binding site is exposed to the extracellular space. Once these molecules bind, the conformation of the transporters change with the glutamate binding site facing the cytoplasm. When the counter-transported K^+ molecule binds to the inward conformation, the conformation changes again so the glutamate binding site is facing the extracellular space (Tzingounis & Wadiche, 2007).

GLT-1 is primarily located on astrocytes and is thought to be responsible for the removal of approximately 90% of glutamate from the extracellular space (Danbolt et al., 1992; Tanaka et al., 1997; Otis & Kavanaugh, 2000). The concentration of GLT-1 at synaptic membranes has been suggested to be regulated by neural activity (Benediktsson et al., 2012). When neural activity is blocked there is a reduction of GLT-1 clusters near synapses, whereas enhanced neural activity increases the size of GLT-1 clusters and their proximity to synapses (Benediktsson et al., 2012). The removal of GLT-1 at synapses, in the timescale of minutes, occurs through endocytosis and is thought to be mediated by protein kinase C (PKC; Robinson, 2006) and ubiquitination, a post-translational

modification, which transfers the protein to recycling endosomes (Martínez-Villarreal et al., 2012). GLT-1 can also be translocated from the recycling endosomes back to the plasma membrane by deubiquitination of the GLT-1 protein (Martínez-Villarreal et al., 2012).

When the gene encoding the GLT-1 protein is knocked out, the resultant elevated level of extracellular glutamate causes lethal seizures in mice (Tanaka et al., 1997). In diseases such as Alzheimer Disease (AD; Li et al., 1997; Hefendehl et al., 2016), epilepsy (Tanaka et al., 1997), and Huntington Disease (HD; Estrada-Sánchez et al., 2009; Huang et al., 2010), it is thought that dysfunctional GLT-1 causes an accumulation of extracellular glutamate which causes a spillover effect and is excitotoxic. Therefore, upregulating GLT-1 expression and/or function is considered to be an important therapeutic strategy in diseases characterized by excessive glutamate levels.

While glutamate transporters, in particular GLT-1, are the focus when researching glutamate clearance, there are many factors other than GLT-1 expression that affect uptake. Recently, it was shown that different brain regions clear glutamate at different efficiencies in response to synaptic activity. The hippocampus was more efficient than both the cortex and striatum at clearing glutamate especially during higher levels of activity where the transporters of the hippocampus seemed less overwhelmed than the other two regions (Pinky et al., 2018). This difference in clearing glutamate based on brain region may be explained by synapse morphology. Chai et al. (2017) used serial electron microscopy to show that astrocytes in the striatum are further away from the post-synaptic density than in the hippocampus. Furthermore, the tortuosity of the

extracellular space can affect clearance by hindering the free diffusion of molecules (Hrabětová, 2005). Finally, if surface mobility of GLT-1 is blocked then glutamate clearance has been shown to be impaired (Murphy-Royal et al., 2015). Therefore, there are many factors that contribute to glutamate clearance efficiency other than overall GLT-1 expression levels.

1.2 Methods to research glutamate dynamics

1.2.1 Microdialysis

Microdialysis is based on the principal of diffusion and the microdialysis probe typically consists of a semipermeable dialysis membrane (Chefer et al., 2009). To measure extracellular levels of a specific neurotransmitter, the no-net-flux method can be used. Artificial cerebral spinal fluid (ACSF) containing several different concentrations of neurotransmitter is perfused into the probe. Next, the amount of neurotransmitter gained to or lost from the probe is measured (Lonnroth et al., 1987; Justice, 1993; Miller et al., 2008). While this method can estimate the ambient concentration of a specific neurotransmitter, microdialysis suffers from poor spatial and temporal resolution.

1.2.2 Synaptically-Activated Transporter Currents

When glutamate is transported across the membrane it causes an influx of positive charge into the cell (Brew & Attwell, 1987), resulting in synaptically-activated transporter currents (STCs) that can be measured by whole-cell patch clamp recordings. Typically, this method is performed on astrocytes and has been used in multiple brain regions including the cortex (Armbruster et al., 2014; Armbruster et al., 2016), hippocampus (Bergles & Jahr, 1997; Diamond & Jahr, 2000), and striatum (Parsons et al.,

2016). However, this technique is time consuming, technically demanding, and is difficult to elicit in brain regions with weak glutamatergic afferents.

1.2.3 Biochemical Uptake Assay

The biochemical uptake assay has been used in neuronal and/or astrocyte cultures or synaptosome preparations (pinched-off nerve endings) to measure exogenous glutamate uptake in various brain regions (Rothstein et al., 1992; Höltje et al., 2008; Huang et al., 2010, Parsons et al., 2016). The biochemical uptake assay involves homogenizing the culture or synaptosomes, incubating the homogenate in exogenous radio-labeled glutamate for several minutes, and measuring the amount of exogenous glutamate incorporated into the homogenate to determine uptake efficiency. While the biochemical uptake assay is perhaps the most commonly used method to measure glutamate uptake, it suffers from poor spatial and temporal resolution. Synaptic morphology is non-existent in this assay and the quantification of uptake relies on the bulk application of exogenous glutamate for several minutes; however, glutamatergic neurotransmission occurs over milliseconds. Finally, it has been suggested that biochemical uptake assays overemphasize the contribution of neuronal uptake in total glutamate transport, thereby questioning their physiological relevance (Petr et al., 2015).

1.2.4 Fluorescent Biosensor of Glutamate

Intensity-based glutamate sensing fluorescent reporter (iGluSnFR) is an extracellular sensor of glutamate which allows the visualization of glutamate dynamics in real-time (Marvin et al., 2013). iGluSnFR was designed as a circular green fluorescent protein (GFP) molecule fused to an extracellular glutamate binding site. At rest, the GFP

fluoresces at a low-intensity and when glutamate binds to iGluSnFR there is a conformational change that increases GFP fluorescence intensity. As well, iGluSnFR can be injected directly into the brain using an adeno-associated virus which infects the cells of the injected brain region with iGluSnFR. It can be expressed under the glial fibrillary acidic protein (GFAP) or synapsin promoter to be selectively expressed in astrocytes or neurons, respectively. When the biochemical uptake assay and iGluSnFR were compared by measuring glutamate clearance in the striatum of both the R6/2 and YAC128 mouse models of Huntington's Disease (HD), it was found that the biochemical uptake assay showed a significant deficit in glutamate clearance; however, iGluSnFR results suggested that there was no deficit in glutamate clearance (Parsons et al., 2016). Therefore, it is important to use a method that keeps synapse morphology intact and allows the visualization of endogenous glutamate clearance. The present thesis uses iGluSnFR to further explore glutamate dynamics in the HD brain.

1.3 An Introduction to Huntington Disease

HD is a progressive neurodegenerative disease characterized by a triad of motor, cognitive, and psychiatric symptoms. This disease is caused by a trinucleotide cytosine-adenine-guanine (CAG) repeat expansion (MacDonald et al., 1993) located on the *Huntingtin (HTT)* gene on chromosome four (Gusella et al., 1983). A normal *HTT* gene typically contains between 10 and 35 CAG repeats which encodes the polyglutamine tract of the resultant huntingtin protein. Individuals with CAG repeats that exceed 35 are at risk of developing HD (Myers et al., 1998); those expressing 36-39 repeats have incomplete penetrance and may or may not develop HD during their lifetime, whereas

individuals with 40 and above repeats show complete penetrance and will develop HD in their lifetime (Brocklebank et al., 2009). Further research showed that the length of CAG repeats is negatively correlated with age of onset (Andrew et al., 1993). While the typical age of onset is around forty years of age (Hayden, 1981), juvenile HD has an age of onset under 20 years old (Andrew et al., 1993).

1.3.1 Symptoms and Treatment

HD is characterized by a triad of motor, cognitive, and psychiatric symptoms. Motor symptoms in HD are considered to be due to the severe neurodegeneration of the striatum, a subcortical brain structure important for motion control. HD patients present with jerky involuntary movements known as chorea. Cognitive deficits commonly occur in spatial working memory, spatial recognition memory, object recognition memory, and episodic memory (Giralt et al., 2012). Psychiatric symptoms usually consist of depression, irritability, increased suicidality, anxiety, and apathy (Paulsen et al., 2001). Although a formal clinical diagnosis is typically not made until overt motor symptoms appear, cognitive and psychiatric symptoms have been shown to appear up to 15 and 20 years before diagnosis, respectively (Duff et al., 2007; Paulsen et al., 2013). Cognitive symptoms are considered by patients and caregivers to be the most debilitating aspect of the disease (Duff et al., 2010; Paulsen, 2011; Paulsen et al., 2013).

Currently, there are only treatments to manage HD symptoms, in particular the motor symptoms. Tetrabenazine (TBZ), a vesicular monoamine transporter, was the first Food and Drug Administration (FDA) approved treatment for HD (Huntington Study Group, 2006). The second FDA-approved treatment for HD was Deutetrabazine (DTBZ)

which is also currently used to help manage the symptoms of chorea (Huntington Study Group, 2016). DBTZ is the same as TBZ except it contains deuterium which extends the metabolic half-life of the drug to decrease the doses HD patients need to take. The efficacy of these drugs is moderate at best, and there are no specific drugs to help treat the cognitive symptoms in HD or to slow overall disease progression. Thus, it is important to increase our understanding of the neurobiology of HD so that better therapeutic targets can be identified.

1.3.2 Mouse models of HD

1.3.2.1 Lesion Models

Lesion models of HD were the first animal models of HD. The excitotoxic animal model of HD involved injecting glutamate analogs (such as kainic acid and quinolinic acid) into the striatum of rats which produced similar histological, neurochemical, and behavioural changes seen in HD (Coyle & Schwarcz, 1976; McGeer & McGeer, 1976). The excitotoxic animal model implicated excessive amounts of glutamate as an important pathophysiology of HD. However, this model causes the quick development of striatal lesions while HD involves slow lesion development over time (Pouladi et al., 2013); therefore, it was important to develop mouse models that more closely recapitulate human HD for preclinical testing of potential treatments.

1.3.2.2 N-Terminal Transgenic Models

Three years after the discovery of the expanded CAG repeat as the cause of HD, the first transgenic mouse model was developed. The R6/1 and R6/2 transgenic mice both express exon 1 of the human HD gene under the human huntingtin promoter, with around

115 and 150 CAG repeats, respectively (Mangiarini et al., 1996). The R6/2 model expresses higher levels of mutant huntingtin and is more aggressive than the R6/1 model. Body tremors develop in R6/1 (Harrison et al., 2013) and R6/2 (Lione et al., 1999) mice at approximately 7 months and 8 weeks of age, respectively. As well, R6/1 mice exhibit cognitive deficits beginning at 12 weeks of age (Nithianantharajah et al., 2008) while the R6/2 mice show learning and memory impairments during cognitive tests such as the Morris water maze starting as early as 3.5 weeks of age, which is the approximate age of puberty in mice (Lione et al., 1999). Furthermore, R6/1 mice develop a depressive-like phenotype at when they have reached mature adulthood, approximately 12 weeks of age (Pang et al., 2008) while R6/2 mice develop anxiety, as shown by elevated plus maze, at approximately 6 weeks of age (File et al., 1998). A caveat of the R6/1 and R6/2 transgenic models is that they only express the N-terminal fragment of the huntingtin protein.

1.3.2.3 Full-length Transgenic Models

The first full-length transgenic HD mouse model was created using yeast artificial chromosome (YAC; Hodgson et al., 1999). YACs containing human genomic DNA containing the full-length HTT gene were introduced to mice. The first YAC HD clones were engineered to contain 46 CAG repeats (YAC46) or 72 CAG repeats (YAC72). The YAC72 model developed a HD-like behavioral phenotype at approximately six months and developed intranuclear aggregates and neurodegeneration in the striatum. At present, the most commonly used YAC model is the YAC128 model. These mice show hyperkinesia at three months, a deficit in rotarod performance at six months of age and

evident striatal atrophy at nine months of age (Slow et al., 2003). As shown in human HD studies, the YAC128 mice also show cognitive deficits and psychiatric symptoms that precede motor deficits.

1.3.2.4 Knock-in Models

Knock-in models of HD have a pathogenic CAG repeat expansion knocked-in to the endogenous murine huntingtin gene and can be homozygous (HOM) or heterozygous (HET) for HD. This is an important aspect when attempting to closely recapitulate the genetics of human HD, as homozygosity for the HD mutation is extremely rare. The zQ175 mouse model of HD is a knock-in model that contains 175 CAG repeats (Menalled et al., 2003; Menalled et al., 2012). At approximately 30 and 38 weeks of age, HOM and HET mice exhibit poor rotarod performance, respectively, indicative of a significant motor deficit (Menalled et al., 2012). When trained in the procedural two-choice swim test, there was only a deficit shown in HOM Q175 mice at 58 weeks of age and no significant performance decline in HET mice (Menalled et al., 2012).

In zQ175 HET mice, the HD-like phenotype is subtle and in some cases, difficult to assess using conventional behavioural tests. To increase phenotypic severity of the zQ175 model, zQ175 mice were backcrossed with FVB/N mice to create the Q175F line (Southwell et al., 2016). Then, mice with cre recombinase were crossed with Q175F mice to excise a neo cassette, which interferes with gene expression (Pham et al., 1996). The end product was the Q175FDN mouse line (Southwell et al., 2016). Similar to the zQ175 model, the Q175FDN mice express the full *HTT* gene. The main difference between the two knock-in models is that the Q175FDN model displays the triad of HD symptoms as

HETs, thereby recapitulating the genetics of human HD. A brief summary of the HD mouse models listed is provided in Table 1.1

1.3.3 Glutamate uptake and GLT-1 in HD

The biochemical uptake assay was used in the R6/2 mice at 8-12 weeks of age and suggested an impairment in glutamate uptake in the striatum and cortex that correlated with a decrease in GLT-1 mRNA and protein expression (Liévens et al., 2001). This change in GLT-1 mRNA expression occurred before any evident neurodegeneration and was suggested to cause an impairment in glutamate uptake. Furthermore, these results were replicated by other researchers who used the biochemical uptake assay (Behrens et al., 2002; Shin et al., 2005; Estrada-Sanchez et al., 2009) and no net-flux microdialysis (Miller et al., 2008). In YAC128 mice there was no reduction in GLT-1 expression but the transporters exhibited reduced palmitoylation, which greatly reduced their efficiency (Huang et al., 2010).

In contrast, when using iGluSnFR and STCs, Parsons et al. (2016) saw no evidence of glutamate uptake impairment in YAC128 mice and even found accelerated glutamate uptake in the R6/2 mouse model. As the biochemical uptake assay involves working with synaptosomes, which has been shown to overemphasize neuronal uptake (Petr et al., 2015), it is important to use a method that can measure glutamate uptake while keeping synapses intact to further explore the excitotoxic hypothesis of HD. Interestingly, a recent study using iGlu_u, an ultrafast sensor of glutamate, found that glutamate uptake in the vicinity of select cortico-striatal axon terminals was indeed

Table 1.1 Summary of HD mouse models. Presented here is an overview of some of the most commonly used HD mouse models summarizing when motor, cognitive, and psychiatric symptoms develop as well as how they express HD.

Mouse Model	Motor Symptoms	Cognitive Symptoms	Psychiatric Symptoms	How HD is Expressed
R6/1	~7 months of age (Harrison et al., 2013)	~3 months of age (Nithianantharajah et al., 2008)	~3 months of age (Pang et al., 2008)	N-terminal fragment only
R6/2	~2 months of age (Lione et al., 1999)	~1-2 months of age (Lione et al., 1999)	~1.5 months of age (File, Mahal, Mangiarini, & Bates, 1998)	N-terminal fragment only
YAC128	~6 months of age (Slow et al., 2003)	~8 months of age (Van Raamsdonk et al., 2005)	~3 months of age (Pouladi et al., 2009)	Yeast artificial chromosome containing 128 CAG repeats
zQ175	HOM: ~8 months; HET: ~9.5 months (Menalled et al., 2012)	HOM: ~13 months; HET: N/A (Menalled et al., 2012)	HOM: ~2 months; HET: ~20 weeks (Menalled et al., 2012)	CAG repeats knocked-in
Q175FDN	HOM: ~6 months; HET: ~8 months (Southwell et al., 2016)	HOM: ~3-6 months; HET: ~6-9 months (Southwell et al., 2016)	HOM: ~3 months; HET: ~6 months (Southwell et al., 2016)	CAG repeats knocked-in without gene suppressing neocassette

impaired in Q175 mice; this effect was replicated in WT mice when both EAAT1 and GLT-1 was blocked (Dvorzhak et al., 2019). There was also a reduction of GLT-1 around the synaptic terminals which is thought to contribute to the glutamate uptake impairment in the Q175 mice (Dvorzhak et al., 2019). However, when GLT-1 was further reduced in the R6/2 model by small interfering RNA (siRNA), there was no increase in disease progression or severity (Petr et al., 2013). In all, the precise contribution of glutamate transporter dysfunction to HD neurobiology remains ambiguous.

1.3.4 Long-Term Potentiation (LTP) and HD

Long-term potentiation (LTP; Bliss & Lømo, 1973) is the activity-dependent strengthening of synapses that underlies the process of learning and memory (Bliss & Collingridge, 1993; Whitlock et al., 2006). The Schaffer collateral pathway (CA1-CA3 synapses) is the most commonly used pathway to study LTP. One form of LTP is NMDAR-dependent LTP which requires the depolarization of the postsynaptic cell to remove the Mg^{2+} from NMDARs. This causes an increase in Ca^{2+} concentration in the post-synaptic cell and activates various intracellular kinases including calmodulin-dependent protein kinase (CaMKII). CaMKII phosphorylates the transmembrane AMPAR regulatory protein (TARP) which causes an increase in synaptic AMPARs (Park et al., 2016).

Two commonly used protocols to induce NMDAR-dependent LTP include high frequency stimulation (HFS) and theta burst stimulation (TBS). HFS is a stimulation protocol consisting of 1 second pulses delivered at 100 Hz (Yun et al., 2002) while TBS typically involves 10 bursts of 4 pulses with 200 ms between each burst (Perez et al.,

1999). Interestingly, when the proteins involved in HFS-LTP and TBS-LTP consolidation were compared, it was found that each protocol required different proteins to induce LTP (Zhu et al., 2015). Thus, numerous patterns of activity can result in NMDAR-dependent LTP through the recruitment of intracellular signaling pathways that are specific to the method of induction.

Up until recent years, the corticostriatal circuit was the focus as the source of cognitive deficits in HD (Bäckman et al., 1997; Cayzac et al., 2011). For example, in pre-symptomatic R6/1 mice, an *in vivo* study measured cell firing in the corticostriatal pathway while the mice performed a procedural learning memory task (Cayzac et al., 2011). These researchers found that there was a diminished recruitment of striatal cells during the task which was associated with cognitive deficits (Cayzac et al., 2011). However, the hippocampus, a brain region involved in learning and memory, also displays significant degeneration in HD human brain tissue (Rosas et al., 2003; Begeti et al., 2016).

Numerous studies have reported LTP deficits in several mouse models of HD. In 1999, Usdin et al. engineered a knock-in mouse model of HD containing approximately 80 CAG repeats and found that these mice exhibited deficits in CA3-CA1 hippocampal LTP compared to WT controls. Furthermore, research evaluating LTP deficits in the R6/2 (Murphy et al., 2000), R6/1 (Giralt et al., 2009), and YAC72 models (Hodgson et al., 1999) all show significant impairments in LTP. Excessive glutamate has been shown to cause LTP deficits (Li et al., 2011) and could be an underlying mechanism of the LTP deficits in HD. Therefore, we sought to uncover if there is a glutamate uptake impairment

in the HD hippocampus and examine if increasing GLT-1 expression may be able to restore LTP deficits to WT levels.

1.4 Pharmacological ways to increase GLT-1 expression

In 2005, Rothstein et al. conducted a blind drug screening to find a pharmaceutical that could increase GLT-1 protein expression. They determined that ceftriaxone, a beta-lactam antibiotic, had the greatest impact on GLT-1 expression and was neuroprotective when used in disease models of Amyotrophic Lateral Sclerosis (ALS) and epilepsy. In a mouse model of AD, ceftriaxone increased GLT-1 expression and glutamate clearance surrounding amyloid beta plaques (Hefendehl et al., 2016). Furthermore, ceftriaxone was able to alleviate motor symptoms in the R6/2 mouse model (Miller et al., 2008). However, its effect on cognitive symptoms in HD has yet to be researched.

Recently, a drug called LDN/OSU-0212320 (LDN) was developed and can also increase GLT-1 protein expression. LDN treatment has been shown to slow disease progression in a mouse model of ALS and prevent the frequency of seizures in a mouse model of epilepsy (Kong et al., 2014). In a mouse model of AD, LDN treatment restored cognitive function and synaptic integrity which continued for up to one month after treatment cessation (Takahashi et al., 2015). Both ceftriaxone and LDN are promising in their ability to upregulate GLT-1 and potentially increase glutamate clearance. However, as described above, transporter expression levels do not necessarily correlate linearly with glutamate uptake rates, and functional glutamate uptake is rarely quantified following ceftriaxone or LDN treatment.

1.5 Aims and Hypothesis

In the present thesis, we used iGluSnFR to demonstrate that under certain patterns of neural activity, a glutamate uptake deficit can be observed in the hippocampus of Q175FDN mice. We hypothesized that ceftriaxone treatment would restore glutamate clearance rates and synaptic plasticity deficits to WT levels. Interestingly, ceftriaxone had no effect on clearance rates in this study. The surprising results of this first study prompted a second study in which we tested the functional effects of ceftriaxone and LDN on glutamate dynamics in multiple brain regions of healthy wild-type mice.

Chapter 2 Materials and Methods

2.1 Animals and Drugs

For experiment 1, we used the Q175FDN knock-in model of HD (N=9; Southwell et al., 2016) and their WT littermates (N=13), both males and females. These mice were bred from 4 breeding pairs at Memorial University in the Animal Care facility using a HET and WT mating paradigm which produces WT (50%) and HET (50%) mice. Mice were housed in ventilated cage racks in groups of 3-4 and kept on a 12:12 light, dark cycle with *ad libitum* food and water. At approximately 5 months of age, stereotaxic surgery was performed on the mice and they were housed separately. Mice in the ceftriaxone (concentration of 10mg/ml) group received intraperitoneal injections of 200mg/kg a day for 7 days while the saline cohort received 0.5-1ml 0.9% saline a day for 7 days.

For experiment 2, 32 WT male FVB mice were ordered from Charles River at 22 days of age. They were housed in ventilated cage racks in groups of 3-4 and kept on a 12:12 light, dark cycle with *ad libitum* food and water. After acclimatization (minimum three days after arrival), stereotaxic surgery was performed on the mice and they were housed separately. Mice were divided into four cohorts: ceftriaxone (N=7), saline (N=7), LDN (N=9), and vehicle (N=9). Mice in the ceftriaxone (concentration of 10mg/ml) group received i.p. injections of 200mg/kg a day for 5-7 days while the saline cohort received 0.5-1ml 0.9% saline a day for 5-7 days. Mice in the LDN group were i.p. injected once with 40mg/kg and the vehicle group injected once with 0.5ml of vehicle

solution (1% Dimethylsulfoxide (DMSO), 1% polyethylene glycol 400, 0.2% Tween 80, 10% hydroxypropyl- β -cyclodextrin. 10% saline).

2.2 Stereotaxic Surgery

For both experiments, mice were anesthetized by isoflurane inhalation (3%) and maintained with 1.5-2% isoflurane for the duration of the surgical procedure. Mice were secured within the ear bars of a standard stereotaxic apparatus (Stoelting), eye drops were used to keep the eyes lubricated throughout the procedure and a 0.5 ml subcutaneous (s.c.) injection of 0.9% sterile saline containing 2 mg/kg meloxicam was provided. When unresponsive to toe-pinch, a small amount of fur above the scalp was cut with a pair of scissors and 0.2 ml of 0.2% lidocaine was injected (s.c) above the skull. A small incision was then made in the scalp around bregma, and the underlying skull was exposed. Next, a hand drill was used to thin the skull at the desired co-ordinates from bregma to expose the underlying cortex while minimizing tissue damage. A Neuros 7002 Hamilton Syringe was attached to an infusion pump (Pump 11 Elite Nanomite, Harvard Apparatus) which was then secured to the stereotaxic frame.

For experiment 1, a total volume of 1 μ l of pAAV.hSyn.iGluSnFr.WPRE.SV40 (syn-iGluSnFR; Addgene, catalogue number 98929-AAV1) was injected into the hippocampus with coordinates of: 2.6 mm posterior, 2.4 mm lateral (right), 1.2 and 1.4 mm ventral to brain surface. We used two ventral coordinates to ensure that the CA3-CA1 region of the hippocampus would be exposed to the virus and express iGluSnFR. At the end of every surgery, the syringe was slowly withdrawn, the incision was sutured and mice were injected with 0.5 ml 0.9% saline (s.c.) before being placed on a heating pad for

approximately 30 minutes to accelerate recovery. For experiment 2, a total volume of 1 μ l of pENN.AAV.GFAP.iGluSnFr.WPRE.SV40 (GFAP-iGluSnFR; Addgene, catalogue number 98930-AAV1) was injected into the cortex, hippocampus, or striatum at an injection rate of 5 nl/s. The syringe was left in place for an additional 5 minutes following the injection. The following co-ordinates were used with respect to bregma: cortex, – 0.7 mm anterior, 2.0 mm lateral (right), 0.6 mm ventral; hippocampus, – 2.6 mm posterior, 2.4 mm lateral (right), 1.2 and 1.4 mm ventral to brain surface; striatum, – 0.7 mm anterior, 2.0 mm lateral (right), 2.6 mm ventral to brain surface.

2.3 Slice Preparation

For experiment 1, mice were aged to 6 months +/- 2 weeks, an age where the HD-phenotype begins to emerge in Q175FDN heterozygous mice (Southwell et al., 2016), and were injected (i.p.) for 7 days with ceftriaxone 2-4 weeks following iGluSnFR injections. For experiment 2, mice were i.p. injected for 5-7 days with ceftriaxone or once with LDN at 2-4 months of age (2-4 weeks following iGluSnFR injections). All mice were anesthetized using isoflurane and decapitated 24 hours after the last injection. The brain was quickly removed and placed in ice-cold oxygenated (95% O₂/5% CO₂) slicing solution consisting of 125mM NaCl, 2.5mM KCl, 25mM NaHCO₃, 1.25mM NaH₂PO₄, 2.5 mM MgCl₂, 1.5mM CaCl₂, 10mM D-(+)-Glucose. Transverse sections (350 μ m) containing the hippocampus and coronal sections (350 μ m) containing the cortex, hippocampus, and striatum were cut using a Leica VT1000 S vibratome for experiment 1 and 2, respectively. Slices were then incubated at room temperature in oxygenated artificial cerebral spinal fluid (ACSF) composed of 125mM NaCl, 2.5mM KCl, 25mM

NaHCO₃, 1.25mM NaH₂PO₄, 1.0mM MgCl₂, 2.0mM CaCl₂, 10mM D-(+)-Glucose.

Slices were left to recover in ACSF for at least 90 or 45 minutes before electrophysiology or imaging experiments, respectively.

2.4 Imaging and image analysis

All slices used for imaging were transferred to a recording chamber under an Olympus BX-61 microscope, and a peristaltic pump (MP-II, Harvard Apparatus) was used to perfuse oxygenated ACSF at a flow rate of 1-2 ml/min. ACSF was heated to 32 °C using an in-line heater and temperature controller (TC-344C, Harvard Apparatus). Glass stimulating electrodes were pulled using a Narishige PB-7 pipette puller to a resistance of 1-2 MΩ when filled with ACSF. The stimulating electrode was placed in the Schaffer collateral (CA3-CA1) pathway within the stratum radiatum of the hippocampus for experiment 1. For experiment 2 the electrode was placed in the deep layers (layer IV and V) of the cortex, the Schaffer collateral pathway of the hippocampus, and in the dorsal part of the striatum. In each experiment, the glass electrode was placed at a depth of approximately 50-100 μm below the slice surface.

Clampex software (Molecular Devices) was used to send TTL triggers through the digital outputs of a Digidata 1550A (Molecular Devices) for precise control over a LED illumination source (Prior, Lumen 300), an EM-CCD camera (Andor, iXon Ultra 897) and an Iso-flex stimulus isolator (AMPI). iGluSnFR responses to evoked neural activity were recorded with Andor Solis software, using 4x4 binning and an acquisition rate of 205 frames per second. For experiment 1, high frequency stimulation (HFS; 100 pulses at 100 Hz) and theta burst stimulation (TBS; 10 bursts of 4 pulses at 50 Hz) each consisted

of one stimulus and one non-stimulus trial with stimulation trials bleach corrected in Fiji. An average of the bleach corrected stimulus trials was created using the IOS and VSD signal processor plugin. For experiment 2, evoked iGluSnFR responses for 2-50 pulses were averaged over 5 trials, with non-stimulus trials interleaved to control for any bleaching of the iGluSnFR signal during acquisition. The non-stimulus trials were averaged in ImageJ and subtracted from the average of the stimulus trials using the IOS and VSD signal processor plugin. For each experiment, the dynamics of extracellular glutamate dynamics within a given field was determined by calculating the average fluorescence intensity within a 10 x 10 pixel ROI (1 pixel at 4x4 binning = 15.6 μm) placed adjacent to the location of the stimulating electrode. Values for $\% \Delta F/F$ were copied to GraphPad Prism and Microsoft Excel for further analysis.

2.5 Electrophysiology for experiment 1 (HFS LTP)

After the recovery period, a slice containing transverse hippocampus was placed in a MED64 multi-electrode probe filled with oxygenated ACSF. The slice was positioned on an 8x8 array of 64 electrodes using a Plugable 250x digital USB camera. Once positioned with electrodes contacting the CA3 and CA1 sub regions of the hippocampus, the probe was placed into the MED64 connector and perfused with oxygenated ACSF run through a peristaltic pump. The slice was left in the system to acclimatize for 15 minutes before stimulation.

After 15 minutes an electrode that was positioned within the Shaffer Collateral projection from CA3-CA1 was selected to be the stimulating electrode. Mobius software was used to monitor responses in the remaining 63 electrodes. An input/output curve was

performed by inducing field excitatory postsynaptic potentials (fEPSP) starting at 10 μ A and increasing in 5 μ A increments to determine the stimulation intensity that elicited 30-40% of the maximal fEPSP response. This stimulation intensity determined from the input/output curve was used to stimulate the slice for plasticity experiments.

The slice was then stimulated with single pulses (0.2 ms width) every 20 seconds. The consequential response was monitored by the remaining 63 electrodes, until a stable baseline was present for 10 consecutive minutes. After a stable baseline was achieved, high frequency stimulation (HFS; Bliss & Collingridge, 1993) was applied to induce long-term potentiation (LTP). HFS consists of 100 pulses in 1 second. fEPSPs were then monitored for 60 minutes following HFS.

2.6 Western Blots

For experiment 1 the hippocampus was dissected from 2 transverse sections (350 μ m each) and for experiment 2 the cortex, hippocampus, and striatum were dissected out and homogenized in 200-400 μ l each of lysis buffer+ containing protease/phosphatase inhibitors. Supernatant was collected from each brain region and protein concentration was determined using BSA standards. 50 μ g of protein from each region was added to separate lanes of 10% SDS PAGE gels for electrophoresis in one times electrophoresis buffer (100 ml of 10 times electrophoresis buffer and 900 ml distilled water) at 100 volts. After the proteins separated on the gel it was placed in one times transfer buffer (100 ml of 10 times transfer buffer, 100 ml of methanol, and 800 ml of distilled water) and was transferred to a nitrocellulose membrane at 100 volts for one hour. The membrane was blocked using 5% milk (5 g of skim milk powder in 100 ml of TBS-T) for one hour. After

blocking, primary antibodies for GLT-1 (E1, 1:1,000, Santa Cruz, mouse-monoclonal) and Actin (C4, 1:1,000, Santa Cruz, mouse-monoclonal) were used, with actin being a loading control and membranes were left in primary antibodies over night at 4 degrees Celsius. The next day, goat anti-mouse IgG-HRP secondary antibody (sc-2005, 1:5,000, Santa Cruz, monoclonal) was added to the membranes and incubated for 1-2 hours at room temperature. Blots were developed using chemiluminescent HRP substrate (Millipore, Cat. No. WBKLS0100, Lot No. 1712501) and ImageJ was used to analyze and quantify the developed bands to determine GLT-1 expression.

2.7 Statistics

Statistical tests, performed in GraphPad Prism, included two-way repeated-measures (RM) ANOVA, and paired *t*-test. The statistical test used for each experiment is indicated in Results. *P* values of <0.05 were considered significant. Where indicated, *N* and *n* refer to the number of animals and slices used in each experiment, respectively.

Chapter 3 Results

3.1 Experiment 1: Treating an animal model of HD with ceftriaxone

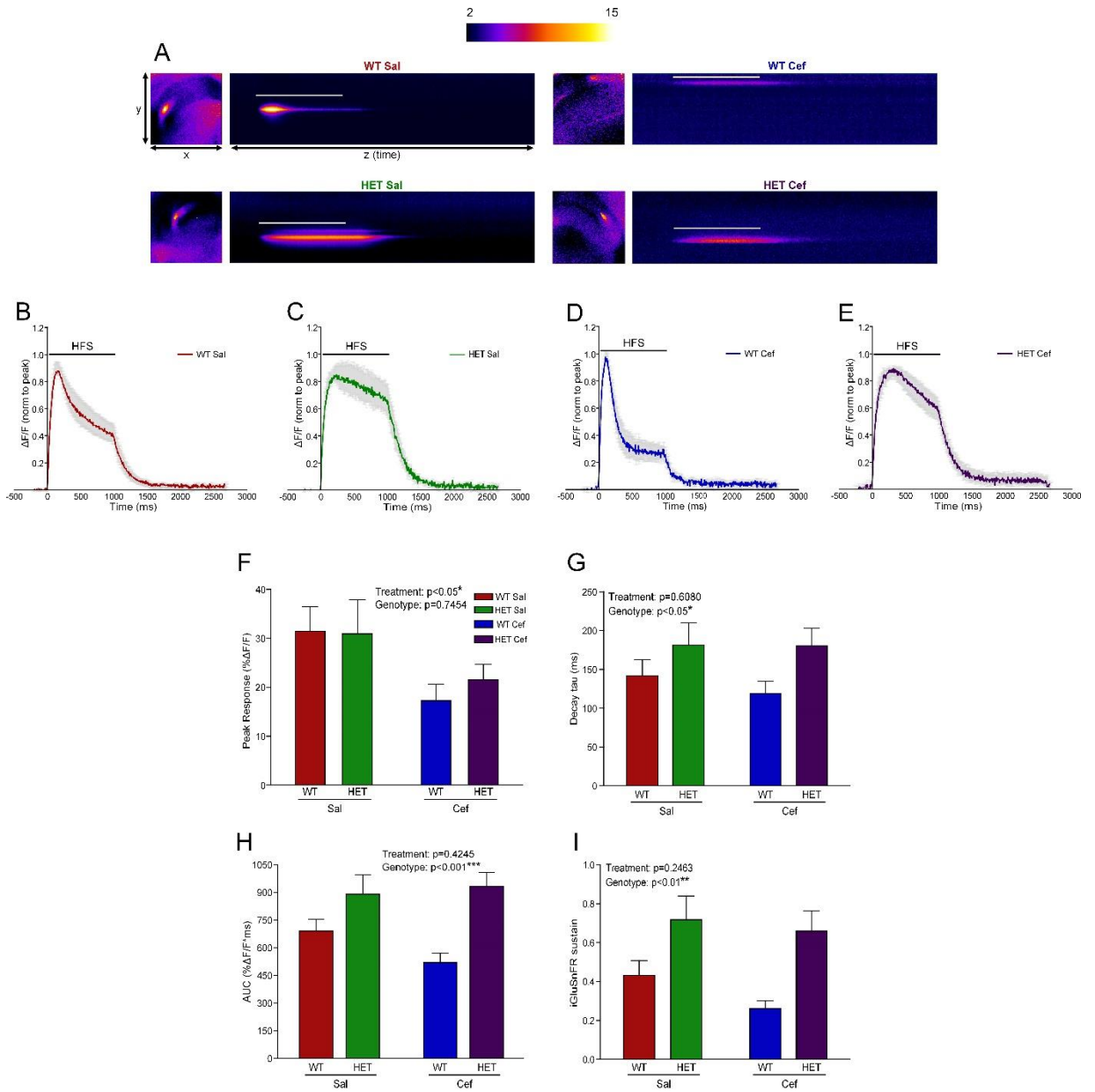
3.1.1 Characterization of extracellular glutamate dynamics in the hippocampus during HFS

We first examined the effect of the HD-causing mutation on glutamate dynamics in the hippocampus as well as the effect of ceftriaxone treatment on glutamate dynamics. To quantify glutamate dynamics during neural activity, we challenged the slices with a high amount of glutamate release by electrically stimulating the Schaffer collateral pathway using HFS (100 pulses, 100 Hz), a commonly-used stimulation paradigm to induce LTP (Fig. 3.1A). Four cohorts of mice were used: WT-Saline (WT-Sal; N=6, n=11; Fig.3.1B), HET-Saline (HET-Sal; N=3, n=6; Fig.3.1C), WT-Cef (N=5, n=6; Fig. 3.1D), and HET-Cef (N=3, n=6; Fig. 3.1E). We expressed iGluSnFR under control of the synapsin promoter to limit iGluSnFR expression to neurons (Marvin et al., 2013); therefore, our study focused on the amount and time-course of endogenous glutamate transients sensed at the neuronal surface in the hippocampus. Glutamate release and clearance rates were visualized in real-time using a high-speed wide field imaging camera (205 Hz) in response to HFS (Fig. 3.1A). The relative magnitude of glutamate release was measured by peak (Koch et al., 2018) which is the maximum $\% \Delta F/F$ (Fig. 3.1F), clearance was measured by calculating the decay tau from the relative decay in fluorescence after stimulation has ended (Pinky et al., 2018; Fig. 3.1G), area under the curve (AUC) reflects the total amount of glutamate accumulation during stimulation (Fig. 3.1 H), and iGluSnFR sustain is how long glutamate stayed in the extracellular space

(Fig. 3.1I). Our results show a significant glutamate clearance impairment in the hippocampus of 6 month old Q175FDN mice (Fig. 3.1G, RM ANOVA, $p_{\text{treatment}}=0.6080$, $p_{\text{genotype}}<0.05$). Furthermore, we found a significant accumulation of glutamate in the Schaffer collateral synapses (AUC; Fig. 3.1H, RM ANOVA, $p_{\text{treatment}}=0.4245$, $p_{\text{genotype}}<0.001$) as well as a significant difference in iGluSnFR sustain (Fig. 3.1I, RM ANOVA, $p_{\text{treatment}}=0.2463$, $p_{\text{genotype}}<0.01$).

Interestingly, we demonstrated that ceftriaxone significantly lowered the peak of glutamate release in both WT and HD treated animals (Fig. 3.1F, RM ANOVA, $p_{\text{treatment}}<0.05$, $p_{\text{genotype}}=0.7454$) with ceftriaxone almost halving the magnitude of glutamate release ($\% \Delta F/F$ values). Conversely, we found that ceftriaxone had no significant effect on decay (Fig. 3.1G, RM ANOVA, $p_{\text{treatment}}=0.6080$), AUC (Fig. 3.1H, RM ANOVA, $p_{\text{treatment}}=0.4245$) or iGluSnFR sustain (Fig. 3.1I, RM ANOVA, $p_{\text{treatment}}=0.2463$) in the hippocampus of WT or HD treated mice. Together, these results suggest there is a buildup of glutamate in the extracellular space in the hippocampus of HD mice that is not prevented by ceftriaxone treatment.

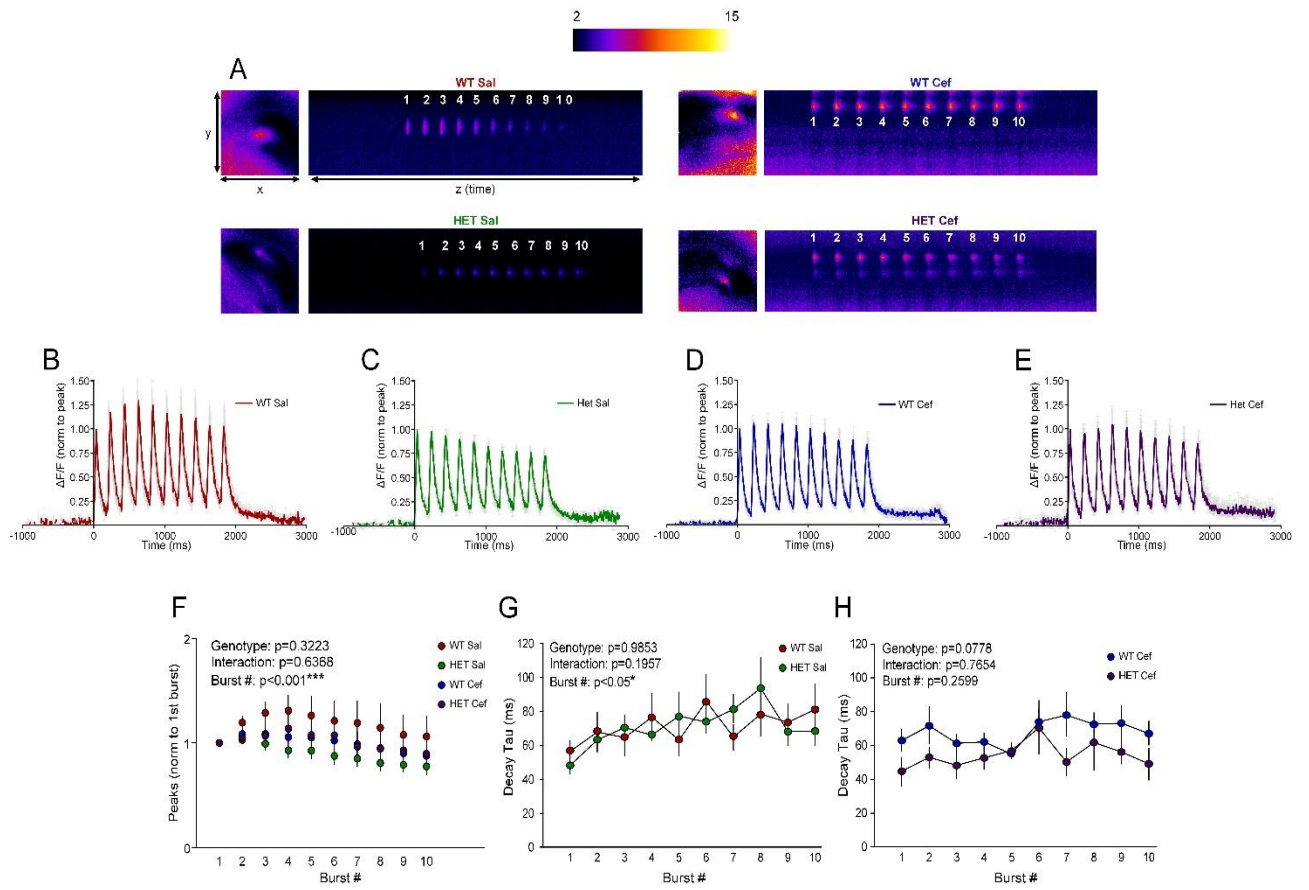
Figure 3.1 Characterization of glutamate dynamics in the hippocampus during HFS. A, representative heat maps of iGluSnFR responses following HFS (100 Hz, 1 s). Maximum projection intensities (peak responses) are shown in the x-y plane (image size = 2 x 2mm), and the y-z (time) plots show the kinetics of the response in the CA1-CA3 projection. The white bar represents the stimulation time. B-E, Mean (\pm SEM) iGluSnFR traces in response to HFS for WT-saline (WT Sal; B), HET-saline (HET Sal; C), WT ceftriaxone (WT Cef; D), and HET ceftriaxone (HET Cef; E). Responses are normalized to their peak. Stimulation time represented by the black bar above the traces. The following graphs are grouped data showing mean (\pm SEM) iGluSnFR response peak (F), decay tau (G), total glutamate accumulation shown by area under the curve (AUC; H), and iGluSnFR sustain, calculated by dividing $\% \Delta F/F$ at the end of stimulation by the peak of the response (I).



3.1.2 Characterization of glutamate dynamics in the hippocampus during TBS

A second commonly used LTP induction protocol is TBS (Larson & Lynch, 1986). While HFS LTP requires adenosine A2A receptors and PKA activation, TBS requires calpain-1 and ERK activation (Zhu et al., 2015). In addition to being modulated by distinct underlying mechanisms, glutamate levels reached during HFS places more pressure on the glutamate transporter system compared to the shorter bursts associated with TBS (Pinky et al., 2018). Therefore, we also used TBS to induce LTP and study glutamate uptake in each group. We stimulated the Schaffer collateral pathway of each group (WT-Sal; N=5, n=6, HET-Sal; N=4, n=7, WT-Cef, N=6, n=8, HET-Cef; N=3, n=5) using TBS (10 bursts of 4 pulses at 100 Hz, inter-burst interval of 200 ms; Fig. 3.2A). We measured responses of each group (Fig. 3.2B-E) and calculated the peak (Fig. 3.2F) and the decay tau at the end of each of the ten bursts associated with TBS (Fig. 3.2G-H). We found no differences in peak between WT and HET mice as well as no interaction effects (Fig. 3.2F, RM ANOVA, $p_{\text{genotype}}=0.3223$, $p_{\text{interaction}}=0.6368$, $p_{\text{burst}}<0.001$). When comparing the decay of WT and HET mice treated with saline, we found no significant genotype or interaction effects (Fig. 3.2G, RM ANOVA, $p_{\text{genotype}}=0.9853$, $p_{\text{interaction}}=0.1957$, $p_{\text{burst}}<0.05$). Similarly, when comparing the decay of WT and HET mice treated with ceftriaxone, there were no significant genotype or interaction effects (Fig. 3.2H, RM ANOVA, $p_{\text{genotype}}=0.0778$, $p_{\text{interaction}}=0.7654$, $p_{\text{burst}}=0.2599$). Our results suggest that while HFS revealed elevated glutamate accumulation and slower clearance rates in the Q175FDN hippocampus, extracellular glutamate dynamics during TBS are not significantly different from those observed in WT mice.

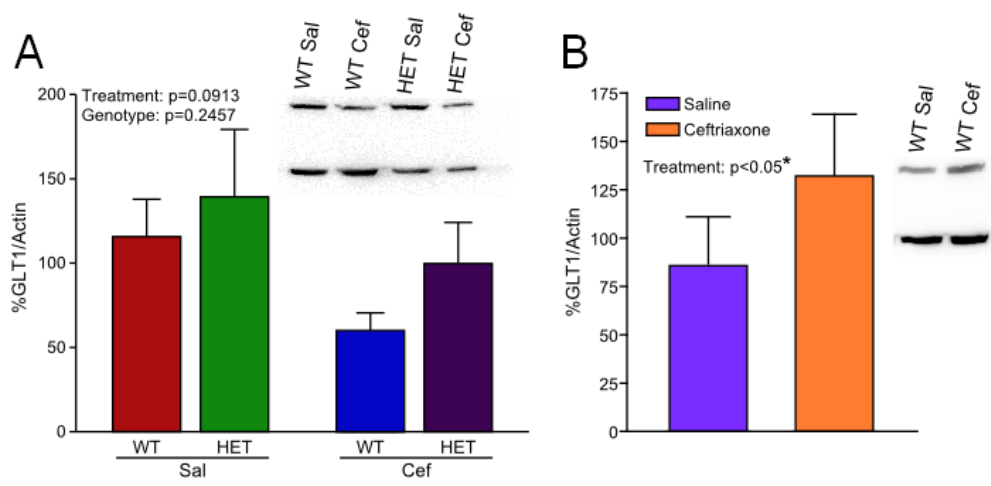
Figure 3.2 Characterization of glutamate dynamics in the hippocampus during TBS. **A**, representative heat maps of iGluSnFR responses following TBS stimulation. Maximum projection intensities (peak responses) are shown in the x-y plane (image size = 2x2mm), and the y-z (time) plots show the kinetics of the response in the CA1-CA3 projection. Burst numbers are above each burst. **B-E**, Mean (\pm SEM) iGluSnFR traces in response to TBS for WT Sal (**B**), HET Sal (**C**), WT Cef (**D**), and HET Cef (**E**). (**F**), grouped data showing mean (\pm SEM) iGluSnFR response peaks. **G-H**, mean (\pm SEM) decay tau results comparing WT Sal and HET Sal (**G**) and WT Cef and HET Cef (**H**).



3.1.3 GLT-1 expression in hippocampal tissue from WT and Q175FDN mice

GLT-1, primarily located on astrocytes, is the brain's most abundant glutamate transporter and makes a substantial contribution to glutamate clearance rates (Danbolt et al., 1992; Tanaka et al., 1997; Otis & Kavanaugh, 2000). To determine whether low GLT-1 expression could explain the alterations in glutamate dynamics observed in Q175FDN hippocampal tissue following HFS, we quantified GLT-1 expression using western blot (WT Sal; N=5, HET Sal; N=5, WT Cef; N=5, HET Cef; N=5). Two-way ANOVA was used to calculate results. We found no significant genotype difference in hippocampal GLT-1 levels (Fig. 3.3A, RM ANOVA, $p_{\text{genotype}}=0.2457$). Surprisingly, we also found that ceftriaxone did not increase GLT-1 expression in either genotype (Fig. 3.3A, RM ANOVA, $p_{\text{treatment}}=0.0913$). As much of the research using ceftriaxone tends to be in younger rats/mice (Rothstein et al., 2005; Miller et al., 2008), we injected a cohort of two-three month old WT mice with either ceftriaxone (N=5) or saline (N=5). In line with previous literature, we found that ceftriaxone treatment significantly increased GLT-1 expression in this cohort of younger, WT mice (Fig. 3.3B, paired t-test; $p_{\text{treatment}}<0.05$). Our results suggest that altered GLT-1 expression is not a cause of altered glutamate dynamics seen in the HD hippocampus following HFS. Furthermore, we have uncovered an age-dependent effect of ceftriaxone at the dose required to increase GLT-1 expression.

Figure 3.3 GLT-1 expression. **(A)** western blot results from 6 month old WT and HET mice injected with either saline or ceftriaxone. **(B)** Western blot results from 2-3 month old WT FVB mice injected with saline or ceftriaxone.



3.1.4 HFS LTP experiments

In addition to quantifying glutamate dynamics, we also asked whether ceftriaxone could restore the LTP impairment known to occur in mouse models of HD (Usdin et al., 1999; Murphy et al., 2000; Giralt et al., 2009). Based on our iGluSnFR imaging results, we found evidence for dysfunctional uptake following HFS but not TBS in the HD hippocampus; therefore, we conducted all LTP experiments using HFS as the induction protocol (WT-Sal; N=3, n=4, HET-Sal; N=3, n=5, WT-Cef; N=5, n=7, HET-Cef; N=5, n=8). We show that in the Q175FDN at this age there was a significant LTP impairment in HD mice (Figure A1, RM ANOVA, $p_{\text{genotype}} < 0.05$). However, we found that ceftriaxone did not improve LTP impairments in HD mice. In fact, ceftriaxone significantly impaired LTP overall (Appendix A, RM ANOVA, $p_{\text{treatment}} < 0.05$). These results suggest that ceftriaxone is not a beneficial treatment to improve LTP deficits and can impair LTP in the healthy brain.

3.2 Experiment 2: Pharmacologically increasing GLT-1 expression in the healthy brain

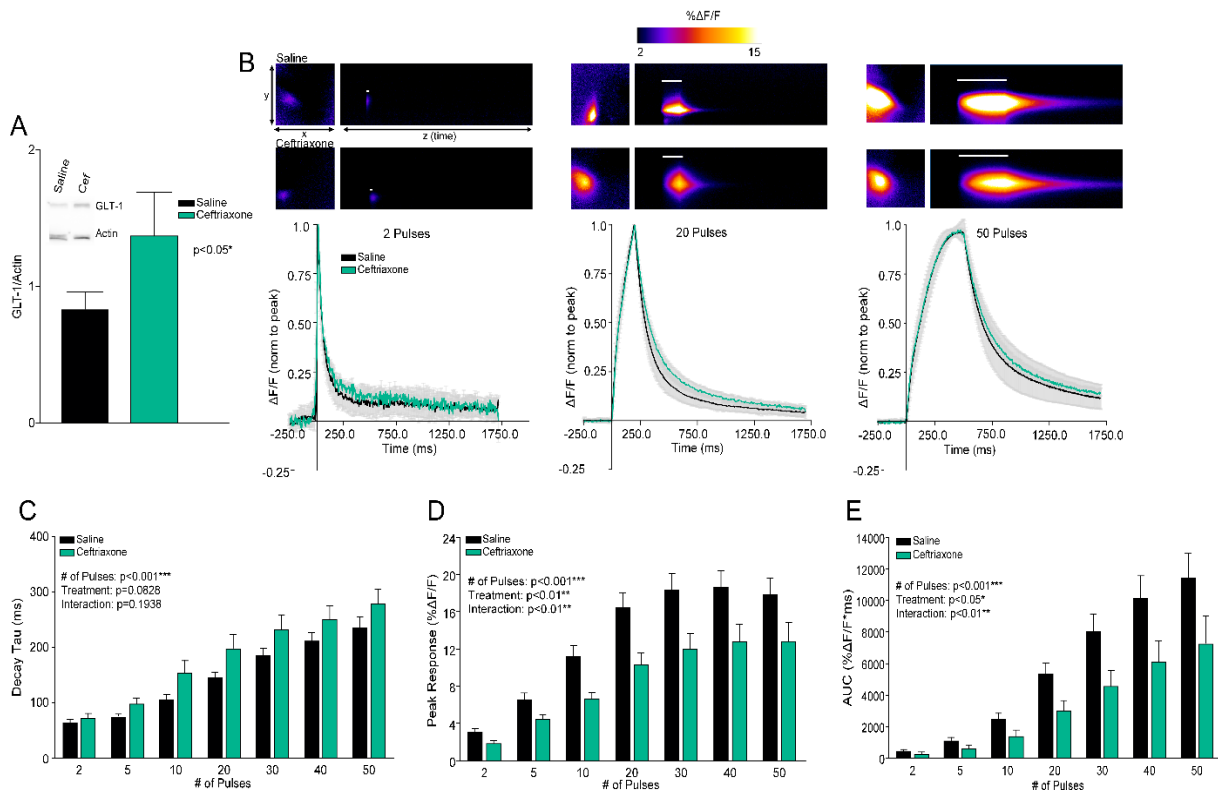
After the completion of Experiment 1, we were surprised to see that ceftriaxone was unable to increase functional measures of glutamate clearance. The hippocampus is already more efficient at clearing glutamate from the extracellular space than other brain regions such as the cortex and striatum (Pinky et al., 2018). Thus, it was of interest to compare the functional effect of increasing GLT-1 expression in the cortex, hippocampus, and striatum in the healthy brain.

3.2.1 Glutamate Clearance in the Cortex after GLT-1 Upregulation

Pinky et al. (2018) demonstrated that glutamate clearance rates vary in an activity- and region-dependent manner. Therefore, we selected three brain regions to study the functional effects of increasing GLT-1 expression. First, we examined the effect of increasing GLT-1 using either ceftriaxone or LDN on glutamate dynamics in the cortex. We injected a cohort of mice with ceftriaxone (N=7, n=16) or saline (N=7, n=16) and found a significant increase in GLT-1 expression after 5-7 days of ceftriaxone treatment (Fig. 3.4A, paired t-test, $p=0.0452$). Next, we stimulated glutamate release (100 Hz) in the deep layers of the cortex with a glass electrode stimulating electrode in control and ceftriaxone treated mice (Fig. 3.4B). As GLT-1 is predominately located on astrocytes, we used the GFAP promoter to limit iGluSnFR expression to astrocytes (Marvin et al., 2013); therefore, our study focuses on the relative amount and time-course of synaptically released glutamate sensed at the astrocytic surface. Glutamate clearance (Fig. 3.4B) was visualized in real-time using a high-speed wide field imaging camera (205 Hz) in response to increasing challenges of glutamate accumulation (2, 5, 10, 20, 30, 40, and 50 pulses; 100 Hz). Despite our observation of a significant increase in GLT-1 expression, we found that ceftriaxone had no significant effect on glutamate clearance rates (Fig. 3.4C, RM Two-way ANOVA, $p_{\text{pulses}} < 0.001$, $p_{\text{treatment}} = 0.0828$, $p_{\text{interaction}} = 0.1938$). While decay taus were not affected, we found that ceftriaxone significantly lowered the response peak (Fig. 3.4D, RM Two-way ANOVA, $p_{\text{pulses}} < 0.001$, $p_{\text{treatment}} = 0.0082$, $p_{\text{interaction}} = 0.0062$) as well as the total amount of glutamate accumulation in the extracellular space, as measured by the area under the curve of iGluSnFR responses (Fig. 3.4E, RM Two-way

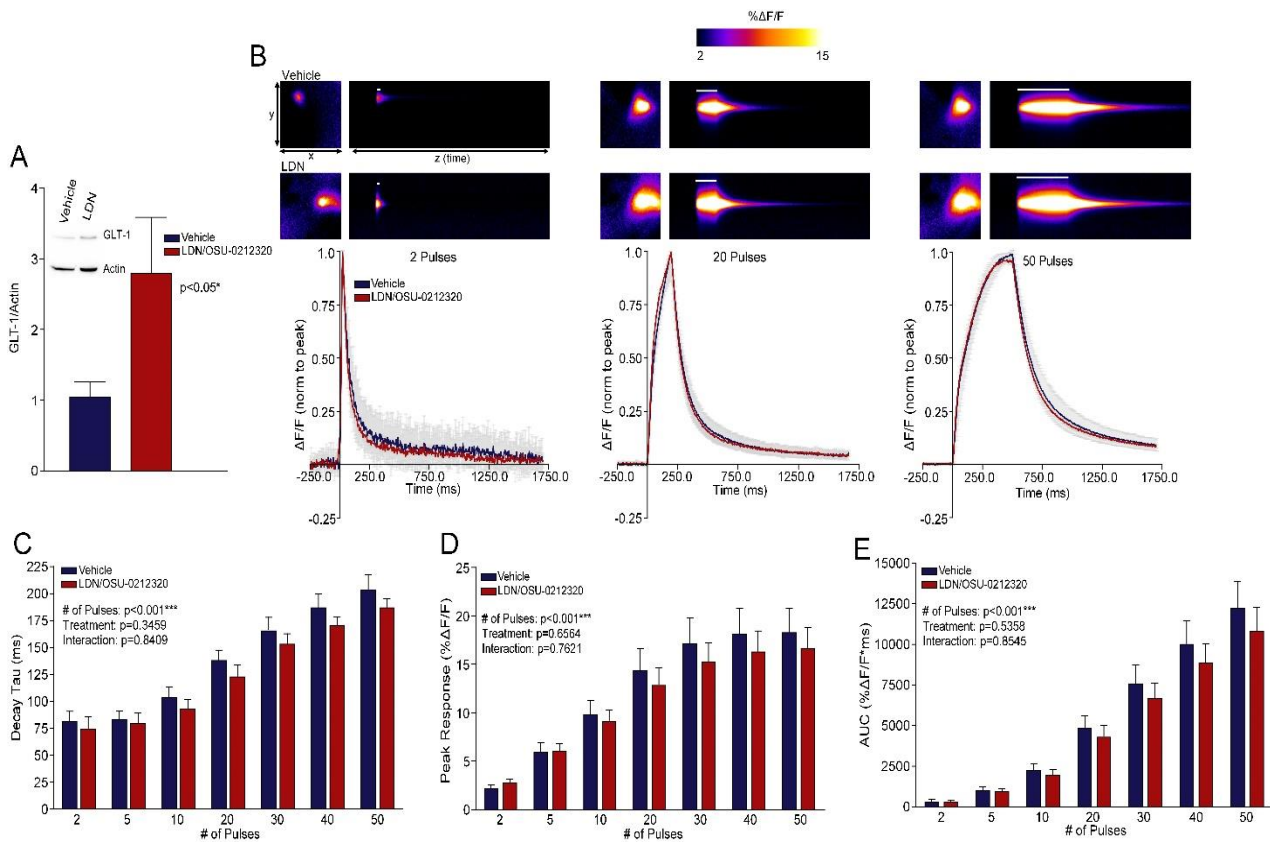
ANOVA, $p_{\text{pulses}} < 0.001$, $p_{\text{treatment}} = 0.0333$, $p_{\text{interaction}} = 0.0044$). Thus, in the cortex, ceftriaxone treatment reduces extracellular glutamate accumulation during neural activity.

Figure 3.4 Characterization of glutamate dynamics in the cortex after ceftriaxone treatment. **A**, western blot results from 2-4 month old male mice injected with either saline (N=7) or ceftriaxone (N=7) for 5-7 days. **B**, representative heat maps and mean (\pm SEM) normalized iGluSnFR responses for 2, 20, and 50 pulses of stimulation (100 Hz). Maximum projection intensities (peak responses) are shown in the x-y plane (image size = 2 x 2mm), and the y-z (time) plots show the kinetics of the response in the deep layers of the cortex. The white bar represents the stimulation time. Mean traces are normalized to peak and black bar represents stimulation time. The following graphs are grouped data showing mean (\pm SEM) iGluSnFR decay tau (**C**), response peak (**D**), and total glutamate accumulation shown by area under the curve (AUC; **E**).



As ceftriaxone had surprisingly little effect on overall glutamate clearance rates, we were interested in assessing another compound known to increase GLT-1 expression, LDN, on glutamate dynamics. In line with previous studies (Kong et al., 2014; Takahashi et al., 2015), we found that, compared to mice injected with vehicle solution (N=9, n=10), LDN (N=9, n=12) significantly increased GLT-1 expression in the cortex (Fig. 3.5A, paired t-test, $p=0.0484$). Again, we stimulated the deep layers of the cortex with a glass stimulating electrode to initiate glutamate release (Fig. 3.5B). Despite the increase in GLT-1 expression, we found that LDN had no significant effect on iGluSnFR decay taus (Fig. 3.5C, RM Two-way ANOVA, $p_{\text{pulses}} < 0.001$, $p_{\text{treatment}} = 0.3459$, $p_{\text{interaction}} = 0.8408$). Unlike ceftriaxone, we found that LDN had no significant effect on the peak (Fig. 3.5D, RM Two-way ANOVA, $p_{\text{pulses}} < 0.001$, $p_{\text{treatment}} = 0.6564$, $p_{\text{interaction}} = 0.7621$) or the area under the curve (Fig. 3.5E, RM Two-way ANOVA, $p_{\text{pulses}} < 0.001$, $p_{\text{treatment}} = 0.5358$, $p_{\text{interaction}} = 0.8545$).

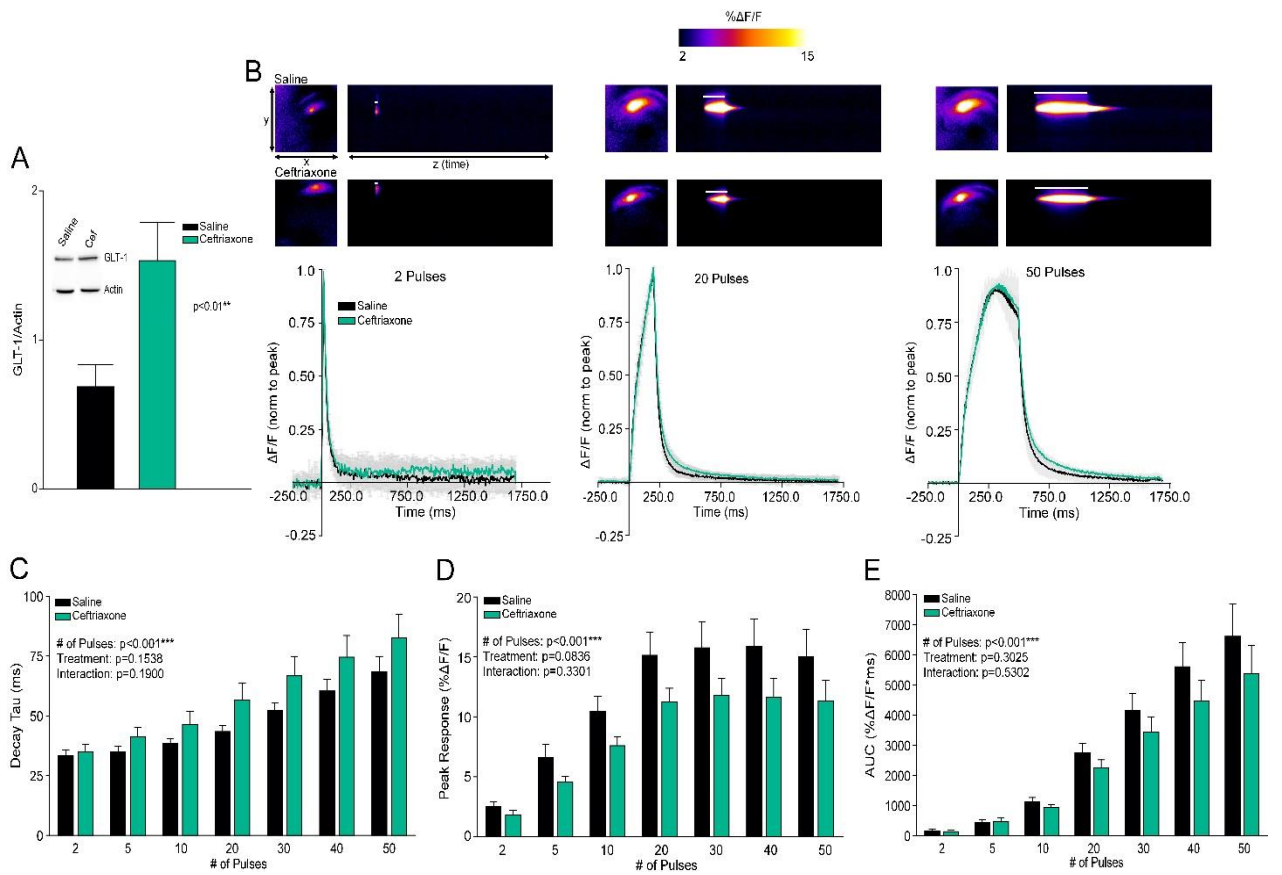
Figure 3.5 Characterization of glutamate dynamics in the cortex after LDN treatment. **A**, western blot results from 2-4 month old male mice injected with either vehicle (N=9) or LDN (N=9) for 1 day. **B**, representative heat maps and mean (\pm SEM) normalized iGluSnFR responses for 2, 20, and 50 pulses of stimulation (100 Hz). Maximum projection intensities (peak responses) are shown in the x-y plane (image size = 2x2mm), and the y-z (time) plots show the kinetics of the response in the deep layers of the cortex. The white bar represents the stimulation time. Mean traces are normalized to peak and black bar represents stimulation time. The following graphs are grouped data showing mean (\pm SEM) iGluSnFR decay tau (**C**), response peak (**D**), and total glutamate accumulation shown by area under the curve (AUC; **E**).



3.2.2 Glutamate Clearance in the Hippocampus after GLT-1 Upregulation

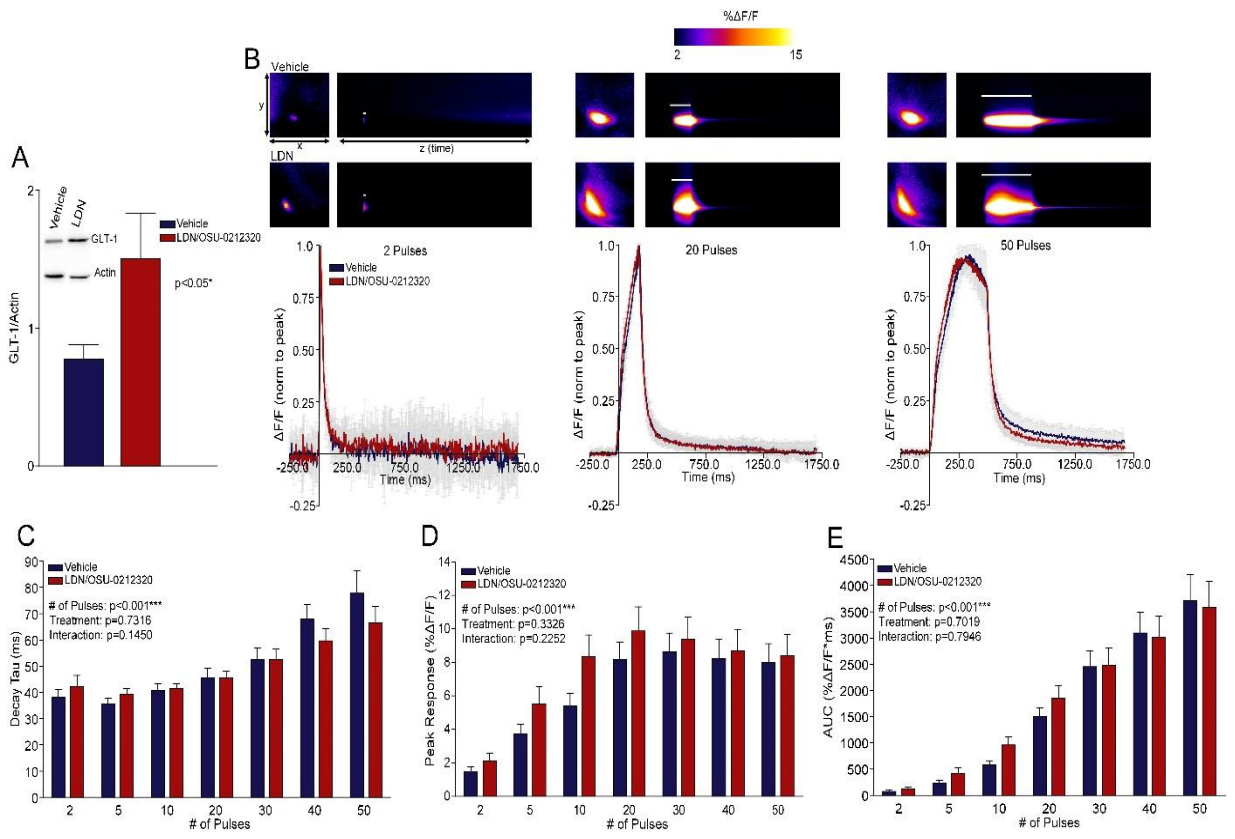
The CA3-CA1 Schaeffer Collateral pathway is the pathway most used to study learning and memory in the brain. First, we injected mice with ceftriaxone to determine how upregulating GLT-1 expression in this area affects glutamate dynamics (Fig. 3.6). We found that, compared to saline (N=7, n=14) injected mice, ceftriaxone (N=7, n=16) significantly increased GLT-1 expression in the hippocampus (Fig. 3.6A, paired t-test, $p=0.0081$). We placed a glass stimulating electrode in the CA3-CA1 area of the hippocampus and stimulated glutamate release using 2, 5, 10, 20, 30, 40, 50 pulses (100 Hz; Fig. 3.6B). Similar to the cortex, we found that ceftriaxone had no significant effect on iGluSnFR decay taus (Fig. 3.6C, RM Two-way ANOVA, $p_{\text{pulses}} < 0.001$, $p_{\text{treatment}} = 0.1538$, $p_{\text{interaction}} = 0.1900$). In addition, ceftriaxone did not significantly affect hippocampal iGluSnFR peaks (Fig. 3.6D, RM Two-way ANOVA, $p_{\text{pulses}} < 0.001$, $p_{\text{treatment}} = 0.0836$, $p_{\text{interaction}} = 0.3301$) or the area under the curve (Fig. 3.6E, RM Two-way ANOVA, $p_{\text{pulses}} < 0.001$, $p_{\text{treatment}} = 0.3025$, $p_{\text{interaction}} = 0.5302$).

Figure 3.6 Characterization of glutamate dynamics in the hippocampus after ceftriaxone treatment. **A**, western blot results from 2-4 month old male mice injected with either saline (N=7) or ceftriaxone (N=7) for 5-7 days. **B**, representative heat maps and mean (\pm SEM) normalized iGluSnFR responses for 2, 20, and 50 pulses of stimulation (100 Hz). Maximum projection intensities (peak responses) are shown in the x-y plane (image size = 2x2mm), and the y-z (time) plots show the kinetics of the response in the CA1-CA3 projection. The white bar represents the stimulation time. Mean traces are normalized to peak and black bar represents stimulation time. The following graphs are grouped data showing mean (\pm SEM) iGluSnFR decay tau (**C**), response peak (**D**), and total glutamate accumulation shown by area under the curve (AUC; **E**).



In LDN-treated mice, we found a significant increase in GLT-1 expression in hippocampal tissue (Fig. 3.7A, paired t-test, $p=0.0496$) when compared to saline-injected mice ($N=9$, $n=13$). Using the same stimulation protocols as above to assess glutamate dynamics (Fig. 3.7B), we found that LDN had no significant effect on iGluSnFR decay taus (Fig. 3.7C, RM Two-way ANOVA, $p_{\text{pulses}} < 0.001$, $p_{\text{treatment}} = 0.7316$, $p_{\text{interaction}} = 0.1450$). There was a trending interaction effect that reflects the tendency for decay taus to be faster following LDN treatment for longer stimulation lengths (e.g. 40 and 50 pulses); however, this did not reach statistical significance. Furthermore, LDN had no significant effect on iGluSnFR peak (Fig. 3.7D, RM Two-way ANOVA, $p_{\text{pulses}} < 0.001$, $p_{\text{treatment}} = 0.3326$, $p_{\text{interaction}} = 0.2252$) or area under the curve in the hippocampus (Fig. 3.7E, RM Two-way ANOVA, $p_{\text{pulses}} < 0.001$, $p_{\text{treatment}} = 0.7019$, $p_{\text{interaction}} = 0.7946$).

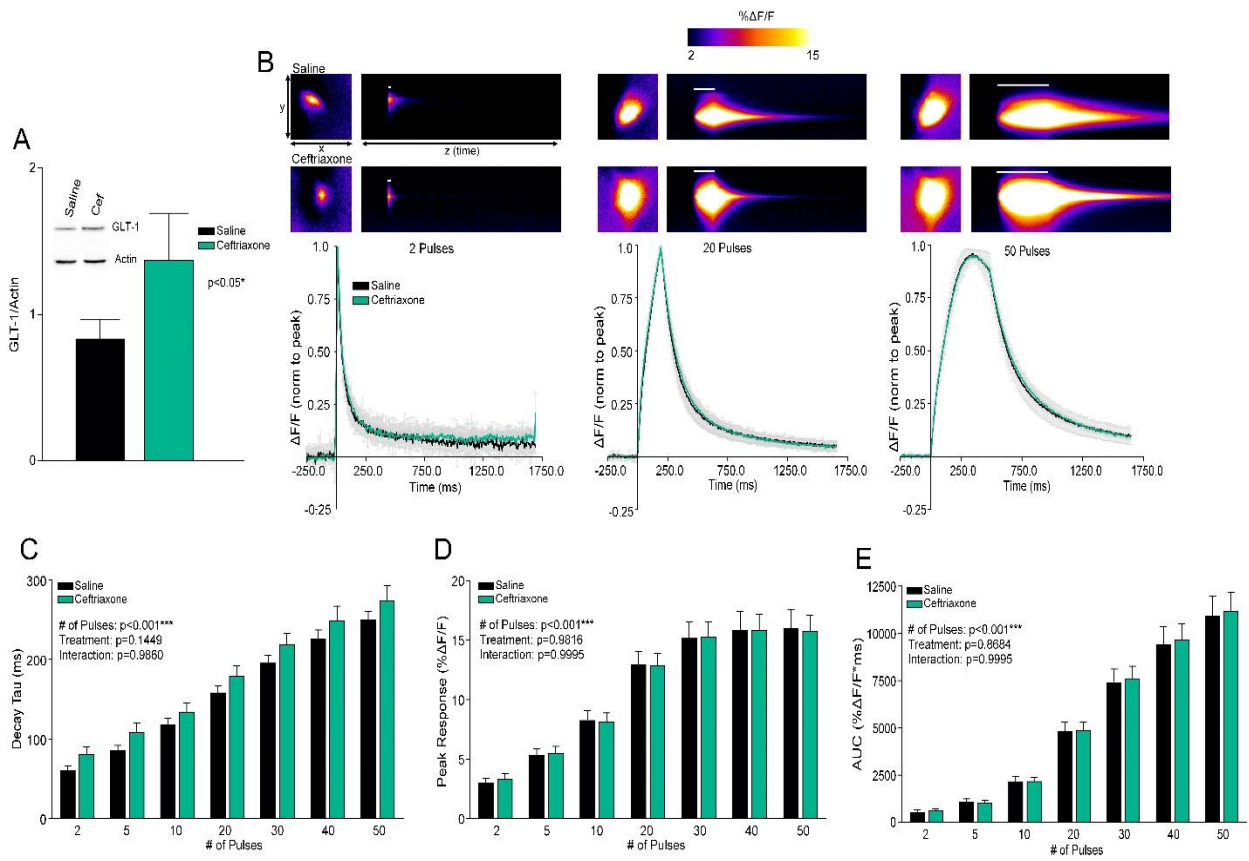
Figure 3.7 Characterization of glutamate dynamics in the hippocampus after LDN treatment. **A**, western blot results from 2-4 month old male mice injected with either vehicle (N=9) or LDN (N=9) for 1 day. **B**, representative heat maps and mean (\pm SEM) normalized iGluSnFR responses for 2, 20, and 50 pulses of stimulation (100 Hz). Maximum projection intensities (peak responses) are shown in the x-y plane (image size = 2x2mm), and the y-z (time) plots show the kinetics of the response in the CA1-CA3 projection. The white bar represents the stimulation time. Mean traces are normalized to peak and black bar represents stimulation time. The following graphs are grouped data showing mean (\pm SEM) iGluSnFR decay tau (**C**), response peak (**D**), and total glutamate accumulation shown by area under the curve (AUC; **E**).



3.2.3 Glutamate Clearance in the Striatum after GLT-1 Upregulation

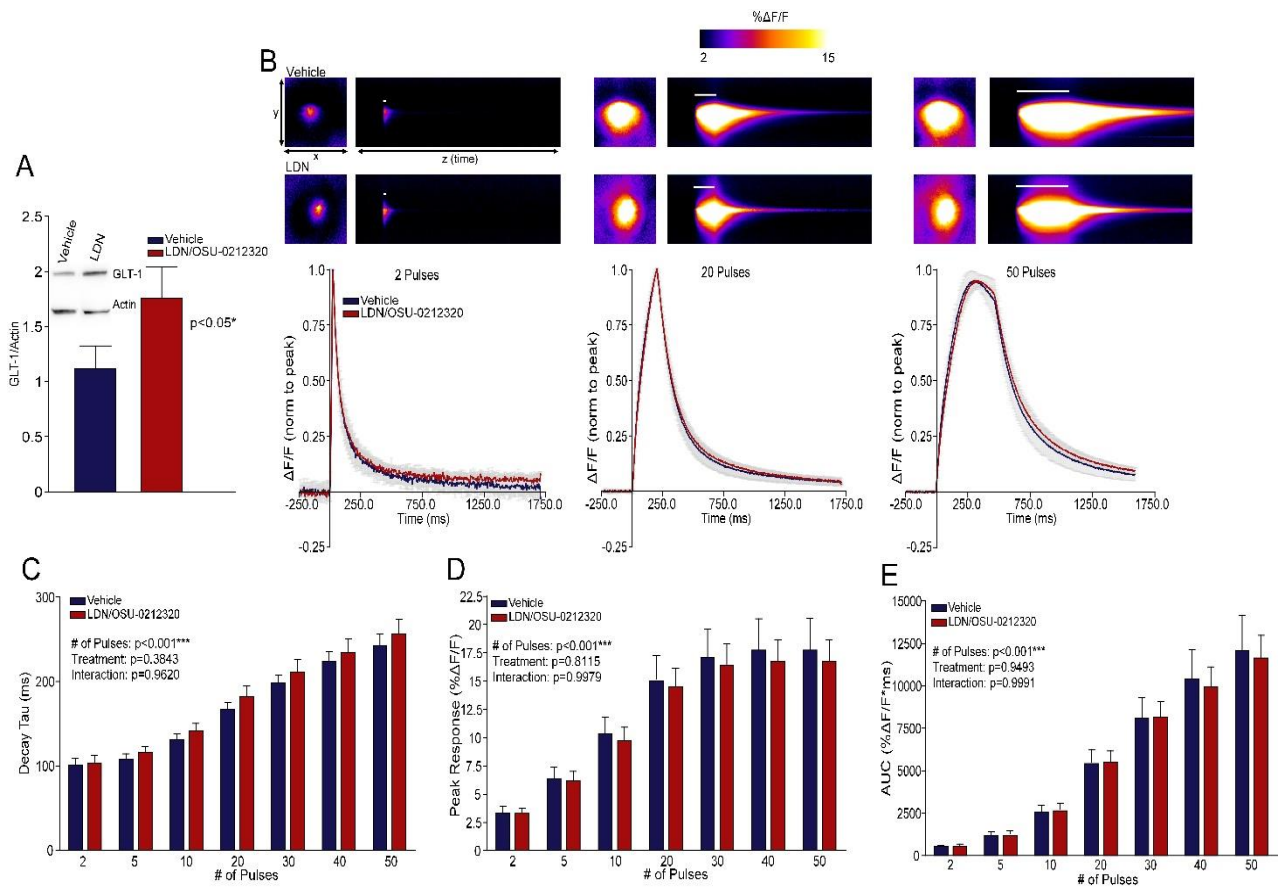
Similar to the cortex and hippocampus, we found that ceftriaxone significantly increased GLT-1 expression in the striatum (Fig. 3.8A, paired t-test, $p=0.0495$, saline; $N=7$, $n=17$, ceftriaxone; $N=7$, $n=20$). We evoked glutamate release in the dorsal striatum by electrical stimulation as before (2, 5, 10, 20, 30, 40, and 50 pulses; 100 Hz; Fig. 3.8B). Similar to the cortex and hippocampus, we found that treatment with ceftriaxone had no significant effect on iGluSnFR decay taus (Fig. 3.8C, RM Two-way ANOVA, $p_{\text{pulses}} < 0.001$, $p_{\text{treatment}} = 0.1449$, $p_{\text{interaction}} = 0.9860$). We also found no significant effects of ceftriaxone on the peak (Fig. 3.8D, RM Two-way ANOVA, $p_{\text{pulses}} < 0.001$, $p_{\text{treatment}} = 0.9816$, $p_{\text{interaction}} = 0.9995$) or total glutamate accumulation, as measured by the area under the curve (Fig. 3.8E, RM Two-way ANOVA, $p_{\text{pulses}} < 0.001$, $p_{\text{treatment}} = 0.8684$, $p_{\text{interaction}} = 0.9995$).

Figure 3.8 Characterization of glutamate dynamics in the striatum after ceftriaxone treatment. **A**, western blot results from 2-4 month old male mice injected with either saline (N=7) or ceftriaxone (N=7) for 5-7 days. **B**, representative heat maps and mean (\pm SEM) normalized iGluSnFR responses for 2, 20, and 50 pulses of stimulation (100 Hz). Maximum projection intensities (peak responses) are shown in the x-y plane (image size = 2x2mm), and the y-z (time) plots show the kinetics of the response in the dorsal striatum. The white bar represents the stimulation time. Mean traces are normalized to peak and black bar represents stimulation time. The following graphs are grouped data showing mean (\pm SEM) iGluSnFR decay tau (**C**), response peak (**D**), and total glutamate accumulation shown by area under the curve (AUC; **E**).



In LDN-treated mice (Fig. 3.9), we also found a significant increase in GLT-1 expression in the striatum (Fig. 3.9A, paired t-test, $p=0.0228$; vehicle; $N=9$, $n=14$, LDN; $N=9$, $n=14$). We used the same stimulation protocol in the dorsal striatum (Fig. 3.9B) and again found no significant effects of LDN on iGluSnFR decay (Fig. 3.9C, RM Two-way ANOVA, $p_{\text{pulses}} < 0.001$, $p_{\text{treatment}} = 0.3843$, $p_{\text{interaction}} = 0.9620$), peak (Fig. 3.9D, RM Two-way ANOVA, $p_{\text{pulses}} < 0.001$, $p_{\text{treatment}} = 0.8115$, $p_{\text{interaction}} = 0.9979$), or area under the curve (Fig. 3.9E, RM Two-way ANOVA, $p_{\text{pulses}} < 0.001$, $p_{\text{treatment}} = 0.9493$, $p_{\text{interaction}} = 0.9991$). In all, these data suggest that increasing GLT-1 expression has a surprisingly little effect on functional measures of glutamate dynamics.

Figure 3.9 Characterization of glutamate dynamics in the striatum after LDN treatment. **A**, western blot results from 2-4 month old male mice injected with either vehicle (N=9) or LDN (N=9) for 1 day. **B**, representative heat maps and mean (\pm SEM) normalized iGluSnFR responses for 2, 20, and 50 pulses of stimulation (100 Hz). Maximum projection intensities (peak responses) are shown in the x-y plane (image size = 2x2mm), and the y-z (time) plots show the kinetics of the response in the CA1-CA3 projection. The white bar represents the stimulation time. Mean traces are normalized to peak and black bar represents stimulation time. The following graphs are grouped data showing mean (\pm SEM) iGluSnFR decay tau (**C**), response peak (**D**), and total glutamate accumulation shown by area under the curve (AUC; **E**).



Chapter 4 Discussion

4.1 Using ceftriaxone to treat the Q175FDN mouse model of HD

Hundreds of studies have used ceftriaxone to increase GLT-1 expression and have used methods such as NMDA currents (Shen et al., 2014), microdialysis (Miller et al., 2008), and the biochemical uptake assay (Shen et al., 2014; Hu et al., 2015) to measure glutamate clearance. In contrast to these methods, iGluSnFR is a useful tool that allows one to directly visualize glutamate dynamics *in situ* in response to different electrical stimulations. Using microdialysis, Miller et al. (2008) found that treating the R6/2 model of HD alleviated motor symptoms; however, the effect of ceftriaxone on cognitive symptoms in HD remain largely unstudied. Cognitive impairments are regarded as the most burdensome symptoms by caregivers and loved ones and can appear 10-15 years before motor symptoms (Paulsen, 2011); therefore, it is imperative to find a possible treatment that could alleviate these cognitive deficits. In our study, we used iGluSnFR and wide-field imaging to study glutamate dynamics in WT and HD animals with and without ceftriaxone treatment during two common LTP induction protocols: HFS (Bliss & Collingridge, 1993) and TBS (Larson & Lynch, 1986).

4.1.1 Glutamate Dynamics in the Hippocampus during HFS and TBS stimulation

We used iGluSnFR to visualize glutamate dynamics in response to synaptic stimulation to demonstrate a glutamate clearance impairment in a brain region involved in learning and memory; the hippocampus. During HFS (100 bursts in 1 second) in HD mice, we saw a significant impairment in glutamate clearance as well as a significant

increase in total glutamate accumulation in the hippocampus which was not alleviated by ceftriaxone treatment. Our results support other studies that show that hippocampal function is affected by the HD-causing mutation (Usdin et al., 1999; Gil et al., 2005; Lynch et al., 2007; Duff et al., 2010; Paulsen et al., 2013; Kolodziejczyk et al., 2014) and may contribute to cognitive deficits associated with HD.

We found that ceftriaxone had an effect on our peak response to HFS by decreasing the maximum amount of glutamate that accumulated in response to trains of electrical stimulation. Recently, it was found that ceftriaxone also upregulates xCT expression (Knackstedt et al., 2010), the catalytic subunit of system xc⁻, which is important in maintaining ambient glutamate levels (Baker et al., 2002). This system pumps out one molecule of glutamate per one molecule of cystine it takes in and this glutamate activates mGluRs 2/3 on the presynaptic membrane (Baker et al., 2002), which has been shown to suppress excitatory neurotransmission (Dietrich et al., 2002). Therefore, in our study, ceftriaxone treatment could be increasing xCT expression and ambient glutamate levels which could be activating presynaptic mGluRs 2/3 and lowering the relative amount of glutamate released in response to HFS. Interestingly, although we observed a ceftriaxone-induced decrease in evoked iGluSnFR peaks, slow glutamate clearance and increased glutamate accumulation was observed in HD mice regardless of treatment, suggesting that glutamate clearance could be dysfunctional in the HD hippocampus and that ceftriaxone treatment has no beneficial effect.

Unlike HFS, we found no genotype differences in glutamate dynamics in response to TBS. While both HFS and TBS result in the release of large amounts of glutamate, the

protocols are different: HFS uses 1 burst of 100 pulses over 1 second while TBS is 10 bursts of 4 pulses every 200 ms for 1 second. It has been shown that glutamate transporters in the hippocampus become overwhelmed at 100 pulses (100 Hz), as seen in HFS, but not at lower pulses such as 5 or fewer pulses, as seen in TBS (Diamond & Jahr, 2000; Pinky et al., 2018). Therefore, even in HD, glutamate transporters may still be functional enough to clear glutamate after lower pulses compared to higher pulses and could explain why no deficiencies in glutamate clearance were found.

4.1.2 Ceftriaxone does not Alleviate LTP Impairments in HD and Impairs LTP in WT Mice

For robust NMDAR-dependent LTP to occur there must be the activation of synaptic NMDARs (Lu et al., 2001). Conversely, activation of extrasynaptic NMDARs can impair LTP (Li et al., 2011) and LTP impairments are frequently shown in mouse models of HD (Usdin et al., 1999; Lynch et al., 2007; Kolodziejczyk et al., 2014). Milnerwood et al. (2010) show that in the early HD striatum of YAC128 mice there is an increase of extrasynaptic NMDAR expression, and the data in the present thesis suggests that HD mice may be vulnerable to excessive glutamate spill-over outside of the synapse during HFS. We demonstrate that in the Q175FDN knock-in model of HD (Southwell et al., 2016), there was an impairment of HFS-induced LTP at 6 months. It is possible that the observed LTP deficit was due to slow glutamate clearance which lead to excessive activation of extrasynaptic NMDARs. Unfortunately, ceftriaxone was unable to restore healthy LTP in Q175FDN mice.

Surprisingly, not only did ceftriaxone fail to restore Q175FDN LTP to control levels, it also impaired LTP in the healthy brain. AMPAR surface diffusion plays an important role in LTP at CA3-CA1 synapses of the hippocampus and if AMPARs are immobilized LTP is impaired (Penn et al., 2017). Ceftriaxone was found to upregulate xCT expression (Knackstedt et al., 2010) which affects postsynaptic AMPA receptor abundance in the hippocampus (Williams & Featherstone, 2014). Therefore, it is possible that at the Schaffer collateral pathway of the hippocampus, ceftriaxone treatment results in the immobilization of AMPARs on the surface of synapses which impairs LTP.

4.1.3 Ceftriaxone did not increase GLT-1 expression in aged animals

Surprisingly, we found that ceftriaxone failed to increase GLT-1 expression in the hippocampus of both WT and HET mice. Past research has shown a decrease in striatal GLT-1 expression that correlates with disease progression in HD mice (Miller et al., 2008; Estrada-Sánchez et al., 2009; Faideau et al., 2010) while other research has shown that GLT-1 protein expression is normal in HD (Huang et al., 2010). In both the striatum and the cortex, Huang et al. (2010) used the biochemical uptake assay to demonstrate a glutamate clearance impairment in the YAC128 model of HD that was not due to altered GLT-1 expression. Instead, these researchers found that GLT-1 was dysfunctional due to reduced palmitoylation of GLT-1. When palmitoylation was inhibited in WT mice they found a decrease in glutamate clearance, showing that palmitoylation is essential for GLT-1 function. We demonstrate that at this age in the hippocampus of Q175FDN mice there is no difference in GLT-1 expression compared to WT mice. Therefore, it is

possible that the altered glutamate dynamics we detected in the HD hippocampus following HFS is a result of GLT-1 depalmitoylation rather than low expression levels.

Finally, we demonstrated an age-dependent effect of ceftriaxone on GLT-1 expression. Most research using ceftriaxone to increase GLT-1 expression uses younger mice; for example, the initial paper by Rothstein et al. (2005) used cultures from postnatal day 9 rats as well as mice aged 70 days old and Miller et al. (2008) used WT and R6/2 mice that were 6 weeks of age. Therefore, we injected a younger WT cohort with saline or ceftriaxone to compare to the 6 month old mice and we found that ceftriaxone increased GLT-1 expression in younger mice. Ceftriaxone upregulates GLT-1 through the activation of nuclear factor-kappa B (NF- κ B) which increases the transcription of the SLC1A2 gene (Lee et al., 2008). As animals get older NF- κ B activation drives the aging process (Adler et al., 2007; Tilstra et al., 2011) and could affect gene transcription. In the hypothalamus in particular, NF- κ B activation contributes to whole organism aging and as the mice grew older NF- κ B activation in the hypothalamus increased (Zhang et al., 2013). Therefore, in the older age we used for our mice, it is possible that aging-induced differences in NF- κ B signaling prevented the typically-observed ceftriaxone-induced increase in GLT-1.

4.2 Pharmacologically increasing GLT-1 expression in the brain

For decades, GLT-1 has been thought to be the most important transporter involved in glutamate clearance and has been suggested to be an important therapeutic target for various neurodegenerative diseases including HD (Miller et al., 2008; Estrada-Sánchez et al., 2009), epilepsy (Tanaka et al., 1997; Petr et al., 2015), and Alzheimer

Disease (Takahashi et al., 2015; Hefendehl et al., 2016). Ceftriaxone and LDN are two compounds capable of upregulating GLT-1 expression and have shown promising results of increasing glutamate clearance (Kong et al., 2014; Shen et al., 2014; Hu et al., 2015). However, these results were obtained using the biochemical uptake assay which has been criticized for lacking physiological relevance (Petr et al., 2015). Furthermore, in the first part of our study, ceftriaxone showed an age-dependent effect on GLT-1 upregulation in WT mice. Therefore, we wanted to understand if increasing GLT-1 expression can increase real-time endogenous glutamate clearance in three different brain regions of younger, WT mice. Here, we use iGluSnFR to visualize glutamate dynamics in real-time after treatment with ceftriaxone or LDN to determine if increasing GLT-1 expression can result in an increase of glutamate clearance in acute brain slices.

4.2.1 Ceftriaxone Treatment to Increase GLT-1 Expression

It has been over a decade since the landmark study conducted by Rothstein et al. (2005) which placed ceftriaxone as the quintessential drug to enhance glutamate clearance for both experimental and/or therapeutic purposes in diseases associated with GLT-1 reduction. Ceftriaxone has shown neuroprotective effects *in vivo* which is thought to be due to its ability to increase GLT-1 expression and, by extension, glutamate clearance. For example, the SOD1(G93) mouse model of amyotrophic lateral sclerosis (ALS), ceftriaxone increased life expectancy and slowed disease progression (Rothstein et al., 2005). However, while most studies report that ceftriaxone treatment is beneficial, there are some studies that have cited no effect or negative side effects. When ceftriaxone was retested in the SOD1(G93A) mouse model, there was no benefit of ceftriaxone

treatment on disease progression (Scott et al., 2008). Furthermore, a clinical trial using ceftriaxone to treat individuals with ALS was stopped as there was no early preclinical efficacy found of the treatment (Cudkowicz et al., 2014). Omrani et al. (2009) found that ceftriaxone treatment significantly impaired long-term depression (LTD), the weakening of synaptic connections, in the mossy fibers of the hippocampus, and a study conducted by Matos-Ocasio et al. (2014) found that treating WT rats with ceftriaxone impaired their performance on the novel object recognition test, a hippocampal-dependent spatial learning task (Barker & Warburton, 2011). Due to these conflicting results, it is important to further understand the functional effects of ceftriaxone treatment throughout the brain.

Surprisingly, we found that ceftriaxone had little effect on iGluSnFR measurements of functional glutamate clearance in multiple brain regions. In fact, there was a slight trend, particularly in the cortex, towards slower glutamate clearance. Slowing glutamate clearance would allow for glutamate to remain in the extracellular space longer which is thought to impair LTP (Li et al., 2011) and lead to cell death (Hardingham & Bading, 2010; Parsons & Raymond, 2014). Huang et al. (2010) found that palmitoylation is an important posttranslational modification that is necessary for GLT-1 to be functional. It is possible that ceftriaxone increased GLT-1 expression by inserting dysfunctional transporters that are missing this important posttranslational modification. If dysfunctional transporters were inserted, rather than clearing glutamate, they could potentially act as a glutamate buffer, thereby delaying clearance. Furthermore, an important aspect of the ability of GLT-1 to clear glutamate is its mobilization across the synapse (Murphy-Royal et al., 2015). When GLT-1 was immobilized, there were slower

kinetics associated with excitatory postsynaptic currents, which could reflect prolonged glutamate times (Murphy-Royal et al., 2015). Therefore, it is also possible that ceftriaxone could be affecting GLT-1 mobilization in each brain region.

An interesting result we uncovered is that ceftriaxone treatment caused a decrease in the peak of the response in the cortex and trended to lower the peak in the hippocampus. It is unlikely that the reduced glutamate accumulation in these cases is a result of more efficient uptake, as accelerated decay kinetics were not observed. Ceftriaxone increases GLT-1 expression transcriptionally by activating the NF- κ B pathway (Lee et al., 2008) which is important in regulating other genes and not just the SLC1A2 gene that encodes for the GLT-1 protein. Recently, it was found that ceftriaxone also upregulates xCT expression (Knackstedt et al., 2010), the catalytic subunit of system xc⁻, which is important in maintaining ambient glutamate levels (Baker et al., 2002). This system pumps out one molecule of glutamate per one molecule of cystine it takes in. The glutamate it pumps out activates mGluRs 2/3 on the presynaptic membrane (Baker et al., 2002) which have been shown to suppress excitatory neurotransmission (Dietrich et al., 2002). Therefore, over the course of ceftriaxone treatment, it is possible that there is an increase in xCT expression and ambient glutamate levels which could be activating presynaptic mGluRs 2/3 and lowering the relative amount of glutamate released in response to stimulation as well as the amount of glutamate accumulation in the extracellular space. Furthermore, with a significant decrease in peak in the cortex we also found a significant decrease in the total amount of glutamate accumulation which, again, can be explained by a potential increase in xCT expression. Our results demonstrate that

upregulating GLT-1 with ceftriaxone in the healthy brain has surprisingly little effect on glutamate dynamics in multiple brain regions and over a wide range of neural activity.

4.2.2 LDN Treatment to Increase GLT-1 Expression

We also used a more recently-developed compound called LDN that increases GLT-1 expression through translational mechanisms (Kong et al., 2014). Kong et al. (2014) treated SOD1(G93A) mice and a pilocarpine-induced mouse model of epilepsy with LDN. In both cases they found that treatment with LDN diminished neuronal degeneration and lowered mortality rate. Furthermore, treatment with LDN in the APP_{Sw,Ind} mouse model of AD significantly improved cognitive function and reduced amyloid beta plaques; these benefits were sustained for one month after treatment (Takahashi et al., 2015). We used iGluSnFR to visualize the effects of LDN on glutamate dynamics in the cortex, hippocampus, and striatum. Interestingly, while LDN increased GLT-1 expression, it had no significant effects on glutamate dynamics in all regions examined. The beneficial results of LDN are thought to be via an increase in glutamate clearance (Kong et al., 2014). However, Kong et al. (2014) used the biochemical uptake assay to demonstrate LDN's ability to increase glutamate clearance. Furthermore, LDN increases GLT-1 translationally by activating protein kinase C (PKC) which activates Y-box binding-1 (YB-1) protein, which has been implicated in interacting with GLT-1 mRNAs (Tanaka et al., 2010). PKC has been shown to increase NMDAR gating and trafficking (Lan et al., 2001) and plays an important role in memory formation (Wang et al., 2006). Furthermore, YB-1 is a multifunctional protein involved in the translational regulation of multiple proteins (Evdokimova et al., 2006). Therefore, any beneficial

effects of LDN treatment could be due to the positive effects of PKC in the brain and subsequent phosphorylation of PKC targets and translational regulation of other proteins due to YB-1 activation. Our results show that LDN treatment was unable to increase glutamate clearance during a wide range of neural activity.

4.3 Conclusion

Using the biochemical uptake assay, it has been shown that ceftriaxone and LDN can increase glutamate uptake due to their beneficial effect of increasing GLT-1 expression. However, we found no beneficial effect of ceftriaxone in the HD hippocampus and also uncovered an age-dependent effect of ceftriaxone on GLT-1 protein expression. As well, in the healthy brain we found no significant effects of ceftriaxone or LDN treatment on glutamate uptake. There are many other factors that affect glutamate uptake such as other transporters, diffusion, other protein such as kir 4.1, as well as posttranslational modifications that affect the functional ability of proteins. Taken together, our results emphasize the importance of testing potential drug interventions at a clinically relevant age in animal models and that accelerating glutamate clearance is much more complex than just simply increasing GLT-1 expression.

Chapter 5 REFERENCES

- Adler, A. S., Sinha, S., Kawahara, T. L., Zhang, J. Y., Segal, E., & Chang, H. Y. (2007). Motif module map reveals enforcement of aging by continual NF-kappaB activity. *Genes and Development, 21*(24), 3244-3257. Retrieved from <http://genesdev.cshlp.org/content/21/24/3244.long>
- Andrew, S. E., Goldberg, Y. P., Kremer, B., Telenius, H., Theilmann, J., Adam, S.,...Hayden, M. R. (1993). The relationship between trinucleotide (CAG) repeat length and clinical features of Huntington's disease. *Nature Genetics, 4*(4), 398-403. DOI: 10.1038/ng0893-398
- Armbruster, M., Hampton, D., Yang, Y., & Dulla, C. G. (2014). Laser-scanning astrocyte mapping reveals increased glutamate-responsive domain size and disrupted maturation of glutamate uptake following neonatal cortical freeze-lesion. *Frontiers in Cellular Neuroscience, 8*(277), 277. <https://doi.org/10.3389/fncel.2014.00277>
- Armbruster, M., Hanson, E., & Dulla, C. G. (2016). Glutamate clearance is locally modulated by presynaptic neuronal activity in the cerebral cortex. *The Journal of Neuroscience, 36*(40), 10404–10415. <https://doi.org/10.1523/JNEUROSCI.2066.16.2016>
- Bäckman, L., Robins-Wahlin, T. B., Lundin, A., Ginovart, N., & Farde, L. (1997). Cognitive deficits in Huntington's disease are predicted by dopaminergic PET markers and brain volumes. *Brain, 120*, 2207-2217. DOI: 10.1093/brain/120.12.2207
- Baker, D. A., Xi, Z. X., Shen, H., Swanson, C. J., & Kalivas, P. W. (2002). The origin

and neuronal function of in vivo nonsynaptic glutamate. *The Journal of Neuroscience*, 22(20), 9134-9141. <https://doi.org/10.1523/JNEUROSCI.22-20-09134.2002>

- Begeti, F., Schwab, L. C., Mason, S. L., & Baker, R. A. (2016). Hippocampal dysfunction defines disease onset in Huntington's disease. *Journal of Neurology, Neurosurgery, & Psychiatry*, 87(9), 975-981. DOI: 10.1136/jnnp-2015-312413
- Behrens, P. F., Franz, P., Woodman, B., Lindenberg, K. S., & Landwehrmeyer, G. B. (2002). Impaired glutamate transport and glutamate-glutamine cycling: Downstream effects of the Huntington mutation. *Brain*, 125(pt. 8), 1908-1922. <https://doi.org/10.1093/brain/awf180>
- Benediktsson, A. M., Marrs, G. S., Tu, J. C., Worley, P. F., Rothstein, J. D., Bergles, D. E., & Dailey, M. E. (2012). Neuronal activity regulates glutamate transporter dynamics in developing astrocytes. *Glia*, 60(2), 175-188. DOI: 10.1002/glia.21249
- Berger, V. U., & Hediger, A. M. (1998). Comparative analysis of glutamate transporter expression in rat brain using differential double in situ hybridization. *Anatomy and Embryology*, 198(1), 13-30. <https://doi.org/10.1007/s004290050161>
- Bergles, D. E., & Jahr, C. E. (1997). Synaptic activation of glutamate transporters in hippocampal astrocytes. *Neuron*, 19(6), 1297-1308. [https://doi.org/10.1016/S0896-6273\(00\)80420-1](https://doi.org/10.1016/S0896-6273(00)80420-1)
- Bliss, T. V., & Collingridge, L. (1993). A synaptic model of memory: Long-term potentiation in the hippocampus. *Nature*, 361, 31-39. Retrieved from <https://www.nature.com/articles/361031a0>

- Bliss, T. V., & Lømo, T. (1973). Long-lasting potentiation of synaptic transmission in the dentate area of the anaesthetized rabbit following stimulation of the perforant path. *The Journal of Physiology*, 232(2), 331-356. Retrieved from <https://www.nature.com/articles/361031a0>
- Brew, H., & Attwell, D. (1987). Electrogenic glutamate uptake is a major current carrier in the membrane of axolotl retinal glial cells. *Nature*, 327, 707–709. <https://doi.org/10.1038/327707a0>
- Brocklebank, D., Gayán, J., Andresen, J. M., Roberts, S. A., Young, A. B., Snodgrass, S. R.,...Cardon, L. R. (2009). Repeat instability in the 27-39 CAG range of the HD gene in the Venezuelan kindreds: Counseling implications. *American Journal of Medical Genetics, Part B, Neuropsychiatric Genetics*, 150B(3), 425-429. DOI: 10.1002/ajmg.b.30826
- Cayzac, S., Delcasso, S., Paz, V., Jeantet, Y., & Cho, Y. H. (2011). Changes in striatal procedural memory coding correlate with learning deficits in a mouse model of Huntington disease. *Proceedings of the National Academy of Sciences of the United States of America*, 108(22), 9280-9285. <https://doi.org/10.1073/pnas.1016190108b>
- Chai, H., Diaz-Castro, B., Shigetomi, E., Monte, E., Oceau, J. C., Yu, X.,...Khakh, B. S. Neural circuit-specialized astrocytes: Transcriptomic, proteomic, morphological, and functional evidence. *Neuron*, 95(3), 531-549. DOI: 10.1016/j.neuron.2017.06.029
- Chefer, V. I., Thompson, A. C., Zapata, A., & Shippenberg, T. S. (2009). Overview of \ brain microdialysis. *Current Protocols in Neuroscience*, 47(1), 1-7.

<https://doi.org/10.1002/0471142301.ns0701s47>

- Clements, J. D., Feltz, A., Sahara, Y., & Westbrook, G. L. (1998). Activation kinetics of AMPA receptor channels reveal the number of functional agonist binding sites. *The Journal of Neuroscience*, *18*(1), 119–127. DOI: 10.1523/JNEUROSCI.18-01-00119.1998
- Colquhoun, D., Jonas, P., & Sakmann, B. (1992). Action of brief pulses of glutamate on AMPA/kainate receptors in patches from different neurones of rat hippocampal slices. *The Journal of Physiology*, *458*(1), 261–287.
<https://doi.org/10.1113/jphysiol.1992.sp019417>
- Cousin, M. A., & Robinson, P. J. (1999). Mechanisms of synaptic vesicle recycling illuminated by fluorescent dyes. *Journal of Neurochemistry*, *73*(6), 2227–2239.
<https://doi.org/10.1046/j.1471-4159.1999.0732227.x>
- Coyle, J. T. & Schwarcz, R. (1976). Lesion of striatal neurones with kainic acid provides a model for Huntington's chorea. *Nature*, *263*(5574), 244-246.
- Cudkovicz, M. E., Titus, S., Kearney, M., Yu, H., Sherman, A., Schoenfeld, D.,...Shefner, J. M. (2014). Efficacy and safety of ceftriaxone for amyotrophic lateral sclerosis: Results of a multi-stage, randomised, double-blind, placebo-controlled, phase 3 study. *The Lancet Neurology*, *13*(11), 1083-1091. DOI: 10.1016/S1474-4422(14)70222-4
- Danbolt, N. C. (2001). Glutamate uptake. *Progress in Neurobiology*, *65*(1), 1-105.
[https://doi.org/10.1016/S0301-0082\(00\)00067-8](https://doi.org/10.1016/S0301-0082(00)00067-8)
- Danbolt, N. C., Storm-Mathisen, J., & Kanner, B. I. (1992). An [Na⁺ + K⁺]coupled L-

- glutamate transporter purified from rat brain is located in glial cell processes. *Neuroscience*, 51(2), 295-310. [https://doi.org/10.1016/0306-4522\(92\)90316-T](https://doi.org/10.1016/0306-4522(92)90316-T)
- Dehnes, Y., Chaudhry, F. A., Ullensvang, K., Lehre, K. P., Storm-Mathisen, J., & Danbolt, N. C. (1998). The glutamate transporter EAAT4 in rat cerebellar Purkinje cells: A glutamate-gated chloride channel concentrated near the synapse in parts of the dendritic membrane facing astroglia. *The Journal of Neuroscience*, 18(10), 3606-3619. <https://doi.org/10.1523/JNEUROSCI.18-10-03606.1998>
- Diamond, J. S. & Jahr, C. E. (2000). Synaptically released glutamate does not overwhelm transporters on hippocampal astrocytes during high-frequency stimulation. *Journal of Neurophysiology*, 83(5), 2835-2843. DOI: 10.1152/jn.2000.83.5.2835
- Dietrich, D., Kral, T., Clusmann, H., Friedl, M., & Schramm, J. (2002). Presynaptic group II metabotropic glutamate receptors reduce stimulated and spontaneous transmitter release in human dentate gyrus. *Neuropharmacology*, 42(3), 297-305. [https://doi.org/10.1016/S0028-3908\(01\)00193-9](https://doi.org/10.1016/S0028-3908(01)00193-9)
- Dore, X. K., Stein, I. S., Brock, X. J. A., Castillo, X. P. E., Zito, X. K., & Sjo, X. P. J. (2017). Unconventional NMDA Receptor Signaling. *The Journal of Neuroscience*, 37(45), 10800–10807. <https://doi.org/10.1523/JNEUROSCI.1825-17.2017>
- Duff, K., Paulsen, J. S., Beglinger, L. J., Langbehn, D. R., & Stout, J. C. (2007). Psychiatric symptoms in Huntington's disease before diagnosis: the predict-HD study. *Biological Psychiatry*, 62(12), 1341-1346. DOI: 10.1016/j.biopsych.2006.11.034

- Duff, K., Paulsen, J., Mills, J., Beglinger, L. J., Moser, D. J., Smith, M. M.,...Harrington, D. L. (2010). Mild cognitive impairment in prediagnosed Huntington disease. *Neurology*, 75(6), 500-507. DOI: 10.1212/WNL.0b013e3181eccfa2
- Dzubay, J. A., & Jahr, C. E. (1996). Kinetics of NMDA channel opening. *The Journal of Neuroscience*, 16(13), 4129-4134. <https://doi.org/10.1523/JNEUROSCI.16-13-04129.1996>
- Estrada-Sánchez, A. M., Montiel, T., Segovia, J., & Massieu, L. (2009). Glutamate toxicity in the striatum of the R6/2 Huntington's disease transgenic mice is age-dependent and correlates with decreased levels of glutamate transporters. *Neurobiology of Disease*, 34(1), 78-86. DOI: 10.1016/j.nbd.2008.12.017
- Evdokimova, V., Ovchinnikov, L. P., & Sorensen, P. H. (2006). Y-box binding protein 1: Providing a new angle on translational regulation. *Cell Cycle*, 5(11), 1143-1147. DOI: 10.4161/cc.5.11.2784
- Faideau, M., Kim, J., Cormier, K., Gilmore, R., Welch, M., Auregan, G.,...Bonvento, G. (2010). In vivo expression of polyglutamine-expanded huntingtin by mouse striatal astrocytes impairs glutamate transport: a correlation with Huntington's disease subjects. *Human Molecular Genetics*, 19(15), 3053-3067. DOI: 10.1093/hmg/ddq212
- Fairman, W. A., Vandenberg, R. J., Arriza, J. L., Kavanaugh, M. P., & Amara, S. G. (1995). An excitatory amino-acid transporter with properties of a ligand-gated chloride channel. *Nature*, 375, 599-603. Retrieved from <https://www.nature.com>
- File, S. E., Mahal, A., Mangiarini, L., & Bates, G. P. (1998). Striking changes in anxiety

- in Huntington's disease transgenic mice. *Brain Research*, 805(1-2), 234-240.
[https://doi.org/10.1016/S0006-8993\(98\)00736-7](https://doi.org/10.1016/S0006-8993(98)00736-7)
- Fonnum, F. (1984). Glutamate: A neurotransmitter in mammalian brain. *Journal of Neurochemistry*, 42(1), 1–11. <https://doi.org/10.1111/j.1471-4159.1984.tb09689.x>
- Gil, J. M. A. C., Mohapel, P., Araújo, I. M., Popovica, N., Lia, J-Y., Brundin, P., & Petersén, Å. (2005). Reduced hippocampal neurogenesis in R6/2 transgenic Huntington's disease mice. *Neurobiology of Disease*, 20(3), 744-751.
<https://doi.org/10.1016/j.nbd.2005.05.006>
- Giralt, A., Saavedra, A., Alberch, J., & Pérez-Navarro, E. (2012). Cognitive dysfunction in Huntington's disease: Humans, mouse models, and molecular mechanisms. *Journal of Huntington's Disease*, 1(2), 155-173. DOI: 10.3233/JHD-120023
- Gusella, J. F., Wexler, N. S., Conneally, P. M., Naylor, S. L., Anderson, M. A., Tanzi, R. E.,...Martin, J. B. A polymorphic DNA marker genetically linked to Huntington's disease. *Nature*, 306, 234-238. Retrieved from www.nature.com
- Hardingham, G. E., & Bading, H. (2010). Synaptic versus extrasynaptic NMDA receptor signalling: Implications for neurodegenerative disorders. *Nature Reviews Neuroscience*, 11(10), 682-696. DOI: 10.1038/nrn2911
- Harrison, D. J., Busse, M., Openshaw, R., Rosser, A. E., Dunnett, S. B., & Brooks, S. P. (2013). Exercise attenuates neuropathology and has greater benefit on cognitive than motor deficits in the R6/1 Huntington's disease mouse model. *Experimental Neurology*, 248, 457-469. <https://doi.org/10.1016/j.expneurol.2013.07.014>
- Hayden, M. R. (1981). *Huntington's Chorea*. Detroit, MI: Springer-Verlag.
- Hefendehl, J. K., LeDue, J., Ko, R. W. Y., Mahler, J., Murphy, T. H., & MacVicar, B. A.

- (2016). Mapping synaptic glutamate transporter dysfunction *in vivo* to regions surrounding A β plaques by iGluSnFR two-photon imaging. *Nature Communications*, 7, 13441. DOI: 10.1038/ncomms13441
- Hestrin, S. (1992). Activation and desensitization of glutamate-activated channels mediating fast excitatory synaptic currents in the visual cortex. *Neuron*, 9(5), 991–999. [https://doi.org/10.1016/0896-6273\(92\)90250-H](https://doi.org/10.1016/0896-6273(92)90250-H)
- Hodgson, J. G., Agopyan, N., Gutekunst, C. A., Leavitt, B. R., LePiane, F., Singaraja, R., ... Hayden, M. R. (1999). A YAC mouse model for Huntington's disease with full-length mutant huntingtin, cytoplasmic toxicity, and selective striatal neurodegeneration. *Neuron*, 23(1), 181-192. [https://doi.org/10.1016/S0896-6273\(00\)80764-3](https://doi.org/10.1016/S0896-6273(00)80764-3)
- Holmseth, S., Dehnes, Y., Huang, Y. H., Follin-Arbelet, V. V., Grutle, N. J., Mylonakou, M. N., ... Danbolt, N. C. (2012). The density of EAAC1 (EAAT3) glutamate transporters expressed by neurons in the mammalian CNS. *The Journal of Neuroscience*, 32(17), 6000–6013. <https://doi.org/10.1523/JNEUROSCI.5347-11.2012>
- Höltje, M., Hofmann, F., Lux, R., Veh, R. W., Just, I., & Ahnert-Hilger, G. (2008). Glutamate uptake and release by astrocytes are enhanced by clostridium botulinum C3 protein. *The Journal of Biological Chemistry*, 283(14), 9289-9299. DOI: 10.1074/jbc.M706499200
- Hrabětová, S. (2005). Extracellular diffusion is fast and isotropic in the stratum radiatum of hippocampal CA1 region in rat brain slices. *Hippocampus*, 15(4), 441-450. <https://doi.org/10.1002/hipo.20068>

- Hu, Y. Y., Xu, J., Zhang, M., Wang, D., Li, L., & Li, W. B. (2015). Ceftriaxone modulates uptake activity of glial glutamate transporter-1 global brain ischemia in rats. *Journal of Neurochemistry*, *132*(2), 194-205. DOI: 10.1111/jnc.12958
- Huang, K., Kang, M. H., Askew, C., Kang, R., Sanders, S. S., Wan, J.,...Hayden, M. R. (2010). Palmitoylation and function of glial glutamate transporter-1 is reduced in the YAC128 mouse model of Huntington disease. *Neurobiology of Disease*, *40*(1), 207-215. DOI: 10.1016/j.nbd.2010.05.027
- Huntington Study Group. (2006). Tetrabenazine as antichorea therapy in Huntington disease: a randomized controlled trial. *Neurology*, *66*(3), 366-372. DOI: 10.1212/01.wnl.0000198586.85250.13
- Huntington Study Group (2016). Effect of Deutetrabenazine on chorea among patients with Huntington disease: A randomized clinical trial. *JAMA*, *316*(1), 40-50. DOI: 10.1001/jama.2016.8655.
- Justice, J. B. Jr. (1993). Quantitative microdialysis of neurotransmitters. *Journal of Neuroscience Methods*, *48*(3), 263-276. [https://doi.org/10.1016/0165-0270\(93\)90097-B](https://doi.org/10.1016/0165-0270(93)90097-B)
- Knackstedt, L. A., Melendez, R. I., & Kalivas, P. W. (2010). Ceftriaxone restores glutamate homeostasis and prevents relapse to cocaine seeking. *Biological Psychiatry*, *67*(1), 81-84. DOI: 10.1016/j.biopsych.2009.07.018
- Koch, E. T., Woodard, C. L., & Raymond, L. A. (2018). Direct assessment of presynaptic modulation of cortico-striatal glutamate release in a Huntington's disease mouse model. *Journal of Neurophysiology*, *120*(6), 3077-3084. DOI: 10.1152/jn.00638.2018

- Kolodziejczyk, K., Parsons, M. P., Southwell, A. L., Hayden, M. R., & Raymond, L. A. (2014). Striatal synaptic dysfunction and hippocampal plasticity deficits in the Hu97/18 mouse model of Huntington disease. *Plos One*, *9*(4).
<https://doi.org/10.1371/journal.pone.0094562>
- Kong, Q., Chang, L. C., Takahashi, K., Liu, Q., Schulte, D. A., Lai, L.,...Lin, C. L. (2014). Small-molecule activator of glutamate transporter EAAT2 translation provides neuroprotection. *Journal of Clinical Investigation*, *124*(3), 1255-1267.
doi: 10.1172/JCI66163
- Lan, J-Y., Skeberdis, V. A., Jover, T., Grooms, S. Y., Lin, Y., Araneda, R. C.,...Zukin, R. S. (2001). Protein kinase C modulates NMDA receptor trafficking and gating. *Nature Neuroscience*, *4*, 382-390. Retrieved from
https://www.nature.com/articles/nn0401_382
- Larson, J., & Lynch, G. (1986). Induction of synaptic potentiation in hippocampus by patterned stimulation involves two events. *Science*, *232*(4753), 985-988. Retrieved from <https://www.ncbi.nlm.nih.gov/pubmed/3704635>
- Lee, S., Su, Z-Z., Emdad, L., Gupta, P., Sarkar, D., Borjabad, A.,...Fisher, P. B. (2008). Mechanism of ceftriaxone induction of excitatory amino acid transporter-2 expression and glutamate uptake in primary human astrocytes. *Journal of Biological Chemistry*, *283*(19), 13116-13123. DOI: 10.1074/jbc.M707697200
- Lester, R. A., & Jahr, C. E. (1992). NMDA channel behavior depends on agonist affinity. *The Journal of Neuroscience*, *12*(2), 635-43.
<https://doi.org/10.1523/jneurosci.6160-08.2009>
- Levy, L. M., Lehre, K. P., Rolstad, B., & Danbolt, N. C. (1993). A monoclonal antibody

raised against an [Na+K+]coupled l-glutamate transporter purified from rat brain confirms glial cell localization, *FEBS Letters*, 317(1-2), 79-84.

[https://doi.org/10.1016/0014-5793\(93\)81495-L](https://doi.org/10.1016/0014-5793(93)81495-L)

Li, S., Jin, M., Koeglsperger, T., Shepardson, N. E., Shankar, G. M., & Selkoe, D. J.

(2011). Soluble A β oligomers inhibit long-term potentiation through a mechanism involving excessive activation of extrasynaptic NR2B-containing NMDA receptors. *Journal of Neuroscience*, 31(18), 6627-6638. DOI:

10.1523/JNEUROSCI.0203-11.2011

Li, S., Mallory, M., Alford, M., Tanaka, S., & Masliah, E. (1997). Glutamate

transporter alterations in Alzheimer disease are possibly associated with abnormal APP expression. *Journal of Neuropathology and Experimental Neurology*, 56(8), 901-911.

Li, S. H., Schilling, G., Young, W. S. 3rd, Li, X. J., Margolis, R. L., Stine, O. C.,...Ross, C. A. (1993). Huntington's disease gene (IT15) is widely expressed in human and rat tissues. *Neuron*, 11(5), 985-993. DOI: 10.1016/0896-6273(93)90127-D

Liévens, J. C., Woodman, B., Mahal, A., Spasic-Bosovic, O., Samuel, D., Kerkerian-Le Goff, L., & Bates, G. P. (2001). Impaired glutamate uptake in the R6 Huntington's disease transgenic mice. *Neurobiology of Disease*, 8(5), 807-821.

<https://doi.org/10.1006/nbdi.2001.0430>

Lione, L. A., Carter, R. J., Hunt, M. J., Bates, G. P., Morton, A. J., & Dunnett, S. B.

(1999). Selective discrimination learning impairments in mice expressing the human Huntington's disease mutation. *Journal of Neuroscience*, 19(23), 10428-

10437. DOI: 10.1523/JNEUROSCI.19-23-10428.1999

- Lonroth, P., Jansson, P. A., & Smith, U. (1987). A microdialysis method allowing characterization of intercellular water space in humans. *American Journal of Physiology*, 253, E228-E231. <https://doi.org/10.1152/ajpendo.1987.253.2.E228>
- Lu, W., Man, H., Ju, W., Trimble, W. S., MacDonald, J. F., & Wang, Y. T. (2001). Activation of synaptic NMDA receptors induces membrane insertion of new AMPA receptors and LTP in cultured hippocampal neurons. *Nature*, 29(1), 243-254. [https://doi.org/10.1016/S0896-6273\(01\)00194-5](https://doi.org/10.1016/S0896-6273(01)00194-5)
- Lynch, G., Kramer, E. A., Rex, C. S., Jia, Y., Chappas, D., Gall, C. M., & Simmons, D. A. (2007). Brain-derived neurotrophic factor restores synaptic plasticity in a knock-in mouse model of Huntington's disease. *The Journal of Neuroscience*, 27(16), 4424-4434. <https://doi.org/10.1523/JNEUROSCI.5113-06.2007>
- MacDonald, M. E., Ambrose, C. M., Duyao, M. P., Myers, R. H., Lin, C. Srinidhi, L.,...Harper, P. S. A novel gene containing a trinucleotide repeat that is expanded and unstable on Huntington's disease chromosomes. *Cell*, 72(6), 971-983. [https://doi.org/10.1016/0092-8674\(93\)90585-E](https://doi.org/10.1016/0092-8674(93)90585-E)
- Man, H. Y. (2011). GluA2-lacking, calcium-permeable AMPA receptors-inducers of plasticity? *Current Opinion in Neurobiology*, 21(2), 291-298. DOI: 10.1016/j.conb.2011.01.001
- Mangiarini, L., Sathasivam, K., Seller, M., Cozens, B., Harper, A., Hetherington, C.,...Bates, G. P. (1996). Exon 1 of the HD gene with an expanded CAG repeat is sufficient to cause a progressive neurological phenotype in transgenic mice. *Cell*, 87(3), 493-506. [https://doi.org/10.1016/S0092-8674\(00\)81369-0](https://doi.org/10.1016/S0092-8674(00)81369-0)
- Martínez-Villarreal, J., García Tardón, N., Ibáñez, I., Giménez, C., & Zafra F. (2012).

- Cell surface turnover of the glutamate transporter GLT-1 is mediated by ubiquitination/deubiquitination. *Glia*, 60(9), 1356-1365. DOI: 10.1002/glia.22354
- Marvin, J. S., Borghuis, B. G., Tian, L., Cichon, J., Harnett, M. T., Akerboom, J.,...Looger, L. L. (2013). An optimized fluorescent probe for visualizing glutamate neurotransmission. *Nature Methods*, 10(2), 162-170. DOI: 10.1038/nmeth.2333
- Matos-Ocasio, F., Hernández-López, A., & Thompson, K. J. (2009). Ceftriaxone, a GLT-1 transporter activator, disrupts hippocampal learning in rats. *Pharmacology, Biochemistry, and Behavior*, 122, 118-121. DOI: 10.1016/j.pbb.2014.03.011
- McGeer, E. G. & McGeer, P. L. Duplication of biochemical changes of Huntington's chorea by intrastriatal injections of glutamic and kainic acids. *Nature*, 263(5577), 517-519. DOI: 10.1038/263517a0
- Menalled, L. B., Sison, J. D., Dragatsis, I., Zeitlin, S., & Chesselet, M-F. (2003). Time course of early motor and neuropathological anomalies in a knock-in mouse model of Huntington's disease with 140 CAG repeats. *Journal of Comparative Neurology*, 465(1), 11-26. DOI: 10.1002/cne.10776
- Menalled, L. B., Kudwa, A. E., Miller, S., Fitzpatrick, J., Watson-Johnson, J., Keating, N.,...Howland, D. (2012). Comprehensive behavioral and molecular characterization of a new knock-in mouse model of Huntington's disease: zQ175. *PLoS One*, 7(12), e49838. DOI: 10.1371/journal.pone.0049838
- Miller, B. R., Dorner, J. L., Shou, M., Sari, Y., Barton, S. J., Sengelaub, D. R....Rebec,

- G. V. (2008). Up-regulation of GLT1 expression increases glutamate uptake and attenuates the Huntington's disease phenotype in the R6/2 mouse. *Neuroscience*, 153(1), 329-337. DOI: 10.1016/j.neuroscience.2008.02.004
- Milnerwood, A. J., Gladding, C. M., Pouladi, M. A., Kaufman, A. M., Hines, R. M., Boyd, J. D.,...Raymond, L. A. (2010). Early increase in extrasynaptic NMDA receptor signaling and expression contributes to phenotype onset in Huntington's disease mice. *Neuron*, 65(2), 178-190. DOI: 10.1016/j.neuron.2010.01.008
- Murphy-Royal, C., Dupuis, J. P., Varela, J. A., Panatier, A., Pinson, B., Baufreton, J.,...Oliet, S. H. (2015). Surface diffusion of astrocytic glutamate transporters shapes synaptic transmission. *Nature Neuroscience*, 18(2), 219-226. DOI: 10.1038/nn.3901
- Myers, R. H., Marans, K., & MacDonald, M.E. (1998). Huntington's disease. In: Warren, S. T., & Well, R. T. (Eds). *Genetic instabilities and hereditary neurological diseases* (pp 301–323). New York, NY: Academic Press.
- Naito, S., & Ueda, T. (1983). Adenosine triphosphate-dependent uptake of glutamate into protein I-associated synaptic vesicles. *Journal of Biological Chemistry*, 258(2), 696-699. Retrieved from www.jbc.org
- Niswender, C. M., & Conn, P. J. (2010). Metabotropic glutamate receptors: Physiology, pharmacology, and disease. *Annual Review of Pharmacology and Toxicology*, 50, 295–322. <https://doi.org/10.1146/annurev.pharmtox.011008.145533>
- Nithianantharajah, J., Barkus, C., Murphy, M., & Hannan, A. J. (2008). Gene-

- environment interactions modulating cognitive function and molecular correlates of synaptic plasticity in Huntington's disease transgenic mice. *Neurobiology of Disease*, 29(3), 490-504. DOI: 10.1016/j.nbd.2007.11.006
- Omrani, A., Melone, M., Bellesi, M., Safiulina, V., Aida, T., Tanaka, K.,...Conti, F. (2009). Up-regulation of GLT-1 severely impairs LTD at mossy fibre-CA3 synapses. *The Journal of Physiology*, 587, 4575-4588. DOI: 10.1113/jphysiol.2009.177881
- Otis, T. S., & Kavanaugh, M. P. (2000). Isolation of current components and partial reaction cycles in the glial glutamate transporter EAAT2. *Journal of Neuroscience*, 20(8), 2749-2757. <https://doi.org/10.1523/JNEUROSCI.20-08-02749.2000>
- Ottersen, O. P., & Storm-Mathisen, J. (1984). Glutamate- and GABA-containing neurons in the mouse and rat brain, as demonstrated with a new immunocytochemical technique. *Journal of Comparative Neurology*, 229(3), 374-392. <https://doi.org/10.1002/cne.902290308>
- Pang, T. Y. C., Du, X., Zajac, M. S., Howard, M. L., & Hannan, A. J. (2008). Altered serotonin receptor expression is associated with depression-related behavior in the R6/1 transgenic mouse model of Huntington's disease. *Human Molecular Genetics*, 18(4), 753-766. <https://doi.org/10.1093/hmg/ddn385>
- Park, J., Chavez, A. E., Mineur, Y. S., Morimoto-Tomita, M., Lutz, S., Kim, K. S.,...Tomita, S. (2016). CaMKII phosphorylation of TARP γ -8 is a mediator of LTP and learning and memory. *Neuron*, 92(1), 75-83. DOI: 10.1016/j.neuron.2016.09.002

- Parsons, M. P., & Raymond, L. A. (2014). Extrasynaptic NMDA receptor involvement in central nervous system disorders. *Neuron*, 82(2), 279-293. DOI: 10.1016/j.neuron.2014.03.030
- Parsons, M. P., Vanni, M. P., Woodard, C. L., Kang, R., Murphy, T. H., & Raymond, L. A. (2016). Real-time imaging of glutamate clearance reveals normal striatal uptake in Huntington disease mouse models. *Nature Communications*, 7(11251). DOI: 10.1038/ncomms11251
- Paulsen, J. S. (2011). Cognitive impairment in Huntington disease: Diagnosis and treatment. *Current Neurology and Neuroscience Reports*, 11(5), 474-483. DOI: 10.1007/s11910-011-0215-x
- Paulsen, J. S., Ready, R. E., Hamilton, J. M., Mega, M. S., & Cummings, J. L. (2001). Neuropsychiatric aspects of Huntington's disease. *Journal of Neurology, Neurosurgery, & Psychiatry*, 71(3), 310-314. <http://dx.doi.org/10.1136/jnnp.71.3.310>
- Paulsen, J. S., Smith, M. M., Long, J. D., & PREDICT-HD. (2013). Cognitive decline in prodromal Huntington Disease: Implications for clinical trials. *Journal of Neurology, Neurosurgery, & Psychiatry*, 84(11), 1233-1239. <http://dx.doi.org/10.1136/jnnp-2013-305114>
- Penn, A. C., Zhang, C. L., Georges, F., Royer, L., Breillat, C., Hosy, E.,...Choquet, D. (2017). Hippocampal LTP and contextual learning require surface diffusion of AMPA receptors. *Nature*, 549, 384-388. DOI: 10.1038/nature23658
- Perez, Y., Chapman, C. A., Woodhall, G., Robitaille, R., Lacaille, J-C. (1999).

Differential induction of long-lasting potentiation of inhibitory postsynaptic potentials by theta patterned stimulation versus 100-Hz tetanization in hippocampal pyramidal cells in vitro. *Neuroscience*, 90(3), 747-757.
[https://doi.org/10.1016/S0306-4522\(98\)00531-4](https://doi.org/10.1016/S0306-4522(98)00531-4)

Petr, G. T., Schultheis, L. A., Hussey, K. C., Sun, Y., Dubinsky, J. M.,...Rosenberg, P. A. (2013). Decreased expression of GLT-1 in the R6/2 model of Huntington's disease does not worsen disease progression. *The European Journal of Neuroscience*, 38(3), 2477-2490. DOI: 10.1111/ejn.12202

Petr, G. T., Sun, Y., Frederick, N. M., Zhou, Y., Dhamne, S. C., Hameed, M. Q.,...Rosenberg, P. A. (2015). Conditional deletion of the glutamate transporter GLT-1 reveals that astrocytic GLT-1 protects against fatal epilepsy while neuronal GLT-1 contributes significantly to glutamate uptake into synaptosomes. *Journal of Neuroscience*, 35(13), 5187-5201. <https://doi.org/10.1523/JNEUROSCI.4255-14.2015>

Pham, C. T., MacIvor, D. M., Hug, B. A., Heusel, J. W., & Ley, T. J. (1996). Long-range disruption of gene expression by a selectable marker cassette. *Proceedings of the National Academy of Sciences of the United States of America*, 93(23), 13090-13095. <https://doi.org/10.1073/pnas.93.23.13090>

Pinky, N. F., Wilkie, C. M., Barnes, J. R., & Parsons, M. P. (2018). Region- and activity-dependent regulation of extracellular glutamate. *The Journal of Neuroscience*, 38(23), 5351-5366. <https://doi.org/10.1523/JNEUROSCI.3213-17.2018>

Pouladi, M. A., Morton, A. J., & Hayden, M. (2013). Choosing an animal model for the

study of Huntington's disease. *Nature Reviews Neuroscience*, *14*(10), 708-721.

DOI: 10.1038/nrn3570

Pouladi, M. A., Graham, R. K., Karasinska, J. M., Xie, Y., Dar Santos, R., Petersén, Å., & Hayden, M. R. (2009). Prevention of depressive behaviour in the YAC128 mouse model of Huntington disease by mutation at residue 586 of huntingtin.

Brain, *132*(4), 919-932. <https://doi.org/10.1093/brain/awp006>

Reiner, A., & Levitz, J. (2018). Glutamatergic signalling in the central nervous system: Ionotropic and metabotropic receptors in concert. *Neuron*, *98*(6), 1080-1098.

<https://doi.org/10.1016/j.neuron.2018.05.018>

Robinson, M. B. (2006). Acute regulation of sodium-dependent glutamate transporters: A focus on constitutive and regulated trafficking. *Handbook of Experimental*

Pharmacology, *175*, 251-275. https://doi.org/10.1007/3-540-29784-7_13

Rosas, H. D., Koroshetz, W. J., Chen, Y. I., Skeuse, C., Vangek, M., Cudkowicz, M.

E.,...Goldstein, J. M. (2003). Evidence for more widespread cerebral pathology in early HD: An MRI-based morphometric analysis. *Neurology*, *60*(10), 1615-

1620. <https://doi.org/10.1212/01.WNL.0000065888.88988.6E>

Rothstein, J. D., Martin, L., Levey, A. I., Dykes-Hoberg, M., Jin, L., Wu, D.,...Kuncl, R.

W. (1994). Localization of neuronal and glial glutamate transporters. *Neuron*,

13(3), 713-725. Retrieved from <https://www.ncbi.nlm.nih.gov/pubmed/7917301>

Rothstein, J. D., Martin, L. J., & Kuncl, R. W. (1992). Decreased glutamate transport by

the brain and spinal cord in amyotrophic lateral sclerosis. *The New England*

Journal of Medicine, *326*, 1464-1468. DOI: 10.1056/NEJM199205283262204

Rothstein, J. D., Patel, S., Regan, M. R., Haenggeli, C., Huang, Y. H., Bergles, D.

- E.,...Fisher, P. B. (2005). Beta-lactam antibiotics offer neuroprotection by increasing glutamate transporter expression. *Nature*, 433(7021), 73-77. Retrieved from <https://www.ncbi.nlm.nih.gov/pubmed/15635412>
- Rothstein, J. D., Van Kammen, M., Levey, a I., Martin, L. J., & Kuncl, R. W. (1995). Selective loss of glial glutamate transporter GLT-1 in amyotrophic lateral sclerosis. *Annals of Neurology*, 38(1), 73–84. <https://doi.org/10.1002/ana.410380114>
- Schmitt, A., Asan, E., Pü, B., & Kugler, P. (1997). Cellular and regional distribution of the glutamate transporter GLAST in the CNS of rats: Nonradioactive in situ hybridization and comparative immunocytochemistry. *The Journal of Neuroscience*, 17(1), 1-10. <https://doi.org/10.1523/JNEUROSCI.17-01-00001.1997>
- Scott, S., Kranz, J. E., Cole, J., Lincecum, J. M., Thompson, K., Kelly, N.,...Heywood, J. A. (2008). Design, power, and interpretation of studies in the standard murine model of ALS. *Amyotrophic Lateral Sclerosis*, 9(1), 4-15. DOI: 10.1080/17482960701856300
- Shashidharan, P., Huntley, G. W., Murray, J. M., Buku, A., Moran, T., Walsh, M. J., ... Plaitakis, A. (1997). Immunohistochemical localization of the neuron-specific glutamate transporter EAAC1 (EAAT3) in rat brain and spinal cord revealed by a novel monoclonal antibody. *Brain Research*, 773(1–2), 139–148. [https://doi.org/10.1016/S0006-8993\(97\)00921-9](https://doi.org/10.1016/S0006-8993(97)00921-9)
- Shen, H. W., Scofield, M. D., Boger, H., Hensley, M., & Kalivas, P. W. (2014). Synaptic

- glutamate spillover due to impaired glutamate uptake mediates heroin relapse. *The Journal of Neuroscience*, 34(16), 5649-5657. DOI: 10.1523/JNEUROSCI.4564-13.2014
- Shin, J. Y., Fang, Z. H., Yu, Z. X., Wang, C. E., Li, S. H., & Li, X. J. (2005). Expression of mutant huntingtin in glial cells contributes to neuronal excitability. *The Journal of Cell Biology*, 171(6), 1001-1012. DOI: 10.1083/jcb.200508072
- Slow, E. J., van Raamsdonk, J., Rogers, D., Coleman, S. H., Graham, R. K., Deng, Y.,...Hayden, M. R. (2003). Selective striatal neuronal loss in a YAC128 mouse model of Huntington disease. *Human Molecular Genetics*, 12(13), 1555-1567. <https://doi.org/10.1093/hmg/ddg169>
- Song, I., & Huganir, R. L. (2002). Regulation of AMPA receptors during synaptic plasticity. *Trends in Neurosciences*, 25(11), 578-588. <https://doi.org/S0166223602022701>
- Southwell, A. L., Smith-Dijak, A., Kay., C., Sepers, M., Villanueva, E. B., Parsons, M. P.,...Hayden, M. R. (2016). An enhanced Q175 knock-in mouse model of Huntington disease with higher mutant huntingtin levels and accelerated disease phenotypes. *Human Molecular Genetics*, 25(17), 3654-3675. <https://doi.org/10.1093/hmg/ddw212>
- Takahashi, K., Kong, Q., Lin, Y., Stouffer, N., Schulte, D. A., Lai, L...Lin, G. (2015). Restored glial glutamate transporter EAAT2 function as a potential therapeutic approach for Alzheimer's disease. *Journal of Experimental Medicine*, 212(3), 319-322. DOI: 10.1084/jem.20140413
- Tanaka, K., Watase, K., Manabe, T., Yamada, K., Watanabe, M., Takahashi, K.,...Wada,

- K. (1997). Epilepsy and exacerbation of brain injury in mice lacking the glutamate transporter GLT-1. *Science*, 276(5319), 1699-1702. DOI: 10.1126/science.276.5319.1699
- Tanaka, T., Ohashi, S., Funakoshi, T., & Kobayashi, S. (2010). YB-1 binds to GluR2 mRNA and CaM1 mRNA in the brain and regulates their translational levels in an activity-dependent manner. *Cellular and Molecular Neurobiology*, 30(7), 1089-1100. DOI: 10.1007/s10571-010-9541-9
- Tilstra, J. S., Clauson, C. L., Niedernhofer, L. J., & Robbins, P. D. (2011). NF- κ B in aging and disease. *Aging and Disease*, 2(6), 449-465. Retrieved from <https://www.ncbi.nlm.nih.gov/pubmed/22396894>
- Traynelis, S. F., Wollmuth, L. P., McBain, C. J., Menniti, F. S., Vance, K. M., Ogden, K. K., ... Dingledine, R. (2010). Glutamate receptor ion channels: structure, regulation, and function. *Pharmacological Reviews*, 62(3), 405-496. <https://doi.org/10.1124/pr.109.002451>
- Tzingounis, A. V., & Wadiche, J. I. (2007). Glutamate transporters: Confining runaway excitation by shaping synaptic transmission. *Nature Reviews Neuroscience*, 8(12), 935-947. <https://doi.org/10.1038/nrn2274>
- Usdin, M. T., Shelbourne, P. F., Myers, R. M., & Madison, D. V. (1999). Impaired synaptic plasticity in mice carrying the Huntington's disease mutation. *Human Molecular Genetics*, 8(5), 839-846. DOI: 10.1093/hmg/8.5.839
- Van Raamsdonk, J. M., Pearson, J., Slow, E. J., Hossain, S. M., Leavitt, B. R., & Hayden,

- M. R. (2005). Cognitive dysfunction precedes neuropathology and motor abnormalities in the YAC128 mouse model of Huntington's disease. *The Journal of Neuroscience*, 25(16), 4169-4180. DOI: 10.1523/JNEUROSCI.0590-05.2005
- Wadiche, J. I., Amara, S. G., & Kavanaugh, M. P. (1995). Ion fluxes associated with excitatory amino acid transport. *Neuron*, 15(3), 721–728. Retrieved from www.cell.com
- Wang, H., Hu, Y., & Tsien, J. Z. (2006). Molecular and systems mechanisms of memory consolidation and storage. *Progress in Neurobiology*, 79(3), 123-135. DOI: 10.1016/j.pneurobio.2006.06.004
- Whitlock, J. R., Heynen, A. J., Shuler, M. G., & Bear, M. F. (2006). Learning induces long-term potentiation in the hippocampus. *Science*, 313(5790), 1093-1097. DOI: 10.1126/science.1128134
- Williams, L. E. & Featherstone, D. E. (2014). Regulation of hippocampal synaptic strength by glial xCT. *Journal of Neuroscience*, 34(48), 16093-16102. <https://doi.org/10.1523/JNEUROSCI.1267-14.2014>
- Yernool, D., Boudker, O., Jin, Y., & Gouaux, E. (2004). Structure of a glutamate transporter homologue from *Pyrococcus horikoshii*. *Nature*, 431(7010), 811–818. <https://doi.org/10.1038/nature03018>
- Yun S. H., Mook-Jung I., Jung M. W. (2002). Variation in effective stimulus patterns for induction of long-term potentiation across different layers of rat entorhinal cortex. *The Journal of Neuroscience*, 22(RC14). <https://doi.org/10.1523/JNEUROSCI.22-05-j0003.2002>
- Zhang, G., Li, J., Purkayastha, S., Tang, Y., Zhang, H., Yin, Y.,...Cai, D. (2013).

Hypothalamic programming of systemic ageing involving IKK- β , NF- κ B and GnRH. *Nature*, 497(7448), 211-216. DOI: 10.1038/nature12143

Zhu, G., Liu, Y., Wang, Y., Bi, X., & Baudry, M. (2015). Different patterns of electrical activity lead to long-term potentiation by activating different intracellular pathways. *The Journal of Neuroscience*, 35(2), 621-633.

<https://doi.org/10.1523/JNEUROSCI.2193-14.2015>

Chapter 6 APPENDIX

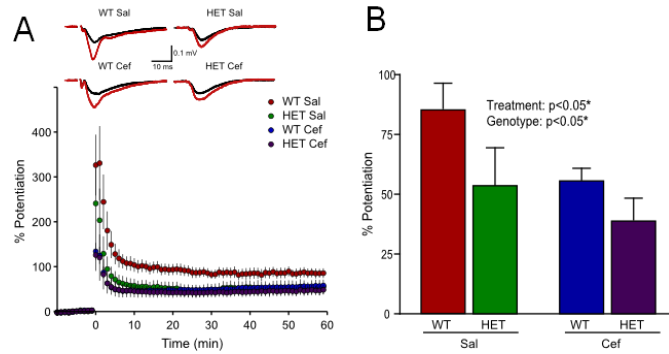


Figure A1: HFS LTP experiments. (A), representative traces and group averages of fEPSP in relation to time. (B) quantification of the fEPSP/time graph. HET mice and WT mice injected with ceftriaxone showed an impairment of percent potentiation, revealing a significant genotype and treatment effect, respectively.